Beta-Glucan Modulates Monocyte Plasticity and Differentiation Capacity to Mitigate DSS-Induced Colitis

Yinyin Lv[#1,3,4], Yanyun Fan[#1,3,4], Qingxiang Gao[#2], Qiongyun Chen[#3,4,6], Yiqun Hu[1,3,4], Lin Wang[1,3,4], Huaxiu Shi[1,3,4], Ermei Chen[1,3,4], Qinyu Xu[1,3,4], Ying Cai[1,3,4], Qingqi Fan[2], Linying Li[2], Dan Du[5], Jianlin Ren[1,3,4*], Shih-Chin Cheng [2,4*], Hongzhi Xu[1,3,4*]

[1]Department of Gastroenterology, The National Key Clinical Specialty, Zhongshan Hospital of Xiamen University, School of Medicine, Xiamen University, Xiamen 361004, Fujian Province, P. R. China

[2]State Key Laboratory of Cellular Stress Biology, School of Life Sciences, Faculty of Medicine and Life Sciences, Xiamen University, Xiamen, Fujian 361102, China

[3]Clinical Research Center for Gut Microbiota and Digestive Diseases of Fujian Province, Xiamen Key Laboratory of Intestinal Microbiome and Human Health，Xiamen 361004, Fujian Province, P. R. China

[4]Department of Digestive Disease, Institute for Microbial Ecology, School of Medicine, Xiamen University, Xiamen 361004, Fujian Province, P. R. China

[5]State Key Laboratory of Cellular Stress Biology, Department of Gastroenterology, Zhongshan Hospital of Xiamen University, School of Medicine, Faculty of Medicine and Life Sciences, Xiamen University, Xiamen 361102, China

[6]Department of Gastroenterology, Taikang Xianlin Drum Tower Hospital, Affiliated Hospital of Medical School, Nanjing University, Nanjing, China

Author contributions: [#]These authors contributed equally work.

[*]Corresponding author:

HongzhiXu (E-mail: xuhongzhi@xmu.edu.cn)

Shih-ChinCheng (E-mail: jamescheng@xmu.edu.cn)

Jianlin Ren (E-mail: jianlin.ren@126.com)

Declaration of interests: The authors declare no competing interests.

Abstract:

Trained immunity involves the reprogramming of innate immune cells after an initial exposure, resulting in heightened inflammatory responses to subsequent stimuli and enhanced bactericidal capacity during infection. However, this proinflammatory state could also exacerbate chronic conditions like inflammatory bowel disease (IBD), which is characterized by persistent inflammation and microbial imbalance. It remains unclear how trained immunity influences IBD pathogenesis and whether it can be harnessed therapeutically. In our study, pretreatment with β-glucan reprogrammed bone marrow hematopoietic progenitors and peripheral monocytes, inducing a profound shift in monocyte plasticity and significantly reducing the severity of dextran sulfate sodium (DSS)–induced colitis. Adoptive transfer of bone marrow or peripheral monocytes from β-glucan–trained mice into naive mice conferred robust protection against colitis, demonstrating that this protective effect is transferable. Trained mice also displayed improved clearance of intestinal bacterial infections. Single-cell RNA sequencing revealed an expansion of reparative Cx3cr1^{+} macrophages derived from Ly6C^{hi} monocytes, correlating with accelerated colonic epithelial regeneration. Collectively, these findings reveal how β-glucan–induced trained immunity modulates monocyte differentiation to ameliorate experimental colitis, highlighting the potential of harnessing trained immunity as a therapeutic strategy to recalibrate innate immune responses and restore gut homeostasis in IBD, shedding light for future clinical applications.

Keywords: Trained immunity, Monocyte/Macrophage, Colitis

Introduction

Inflammatory bowel disease (IBD), encompassing ulcerative colitis (UC) and Crohn's disease (CD), is a chronic gastrointestinal inflammatory disorder associated with significant morbidity(1, 2). The intestinal mucosa is continuously exposed to a diverse microbial ecosystem, including fungi, bacteria, and viruses(3). In IBD, the delicate balance between the immune system and the microbiota is disrupted, leading to uncontrolled inflammation(4, 5). This dysregulation is further exacerbated by genetic factors, such as loss-of-function mutations in NOD2, which impair antimicrobial peptide production, increase susceptibility to intestinal infections, and decrease IL-10 production by monocytes(6-8).

Trained immunity, a phenomenon where innate immune cells exhibit enhanced responses to secondary challenges, has emerged as a promising therapeutic avenue for various infectious diseases and cancer(9-13). However, its role in chronic inflammatory conditions like IBD remains largely unexplored. While trained immunity can enhance pathogen clearance, it also involves the upregulation of pro-inflammatory cytokines such as TNF, IL-1β, and IL-6(14), therefore the role of trained immunity in IBD remained elusive.

This study aimed to investigate the therapeutic potential of trained immunity in a mouse model of colitis. We hypothesized that inducing trained immunity could enhance microbial control, thereby preserving intestinal integrity and ultimately mitigating disease severity. To test this, we employed β-glucan (BG), a prototypic trained immunity inducer, and assessed its impact on dextran sulfate sodium (DSS)-induced colitis. Our findings demonstrate that BG pretreatment significantly alleviates colitis in mice. Mechanistically, BG induced central immunity in the hematopoietic compartment, leading to the generation of "trained" monocytes in the periphery. Both bone marrow transplantation from trained donors and adoptive transfer of trained monocytes conferred protection against DSS-induced colitis. Furthermore, single-cell RNA-seq revealed that BG-induced trained immunity promotes the expansion of reparative Cx3cr1 intestinal macrophages derived from Ly6C^{hi} monocytes, thereby facilitating epithelial regeneration. In summary, our data suggest that harnessing trained immunity represents a promising therapeutic approach for IBD treatment.

Results

β-glucan (BG) pretreatment ameliorates DSS-induced colitis

To investigate the impact of trained immunity on colitis, mice were pretreated with BG, a potent inducer of trained immunity. Successful induction of BG-induced trained immunity (BGTI) was confirmed by the enhanced resistance to *Staphylococcus aureus* infection in BG-treated mice (**Fig S1A and S1B**), consistent with previous findings(15). Importantly, BG-pretreatment did not induce spontaneous intestinal inflammation (**Fig S1C and S1D)**. Following BGTI induction, mice were subjected to DSS-induced colitis. (**Fig 1A**). BG pretreatment significantly ameliorated disease severity, as indicated by the reduced body weight loss (**Fig 1B and Fig S1E**), colon shortening (**Fig 1C and Fig S1F and S1G**), and diminished mucosal inflammation observed via endoscopic imaging (**Fig 1D**). Histological analysis demonstrated lower histopathologic scores (**Fig 1E and 1F**). Additionally, BG-pretreated mice exhibited enhanced intestinal epithelial barrier integrity, as evidenced by the increased expression of tight junction proteins Zo-1 and Occludin (**Fig 1G and 1H**), and decreased circulating FITC-dextran levels (**Fig 1I**).

Acknowledging that the long-lasting effects of BGTI(16), we further examined its long-term protective effects against DSS-induced colitis. Despite peripheral myeloid cells and monocytes returning to homeostasis four weeks post-BG treatment (**Fig S2A and S2B**), mice remained protected against DSS-induced colitis as demonstrated by body weight change and colon shortening (**Fig 1J and 1K**), and improved histological outcomes (**Fig S2C and S2D**). This BG-induced protection persisted for up to seven weeks (**Fig S2E and S2F**). These findings indicate that BG pretreatment effectively ameliorates DSS-induced colitis in mice, emphasizing the therapeutic potential of trained immunity in IBD management.

BG ameliorates colitis via enhanced myeloid cell activation independent of adaptive immunity

Given that BGTI has been reported to function independently of adaptive immunity(17, 18), we evaluated the effects of BG pretreatment in *Rag1* knockout mice (**Fig S3A-S3D**). Notably, BG pre-treatment remained effective in *Rag1*$^{-/-}$ mice, as evidenced by reduced body weight loss, colon

shortening, and improved histological outcomes (**Fig S3E-S3H**). These findings confirm that BGTI-mediated protection is independent of adaptive immune responses, consistent with previous findings demonstrating that adaptive immunity is dispensable for trained immunity.

To gain a comprehensive understanding of the molecular mechanisms underlying BG-mediated protection, we performed RNA sequencing on colonic samples collected at multiple time points following DSS administration. WGCNA identified the MEturquoise module emerged as the core functional module, containing 5,015 genes whose expression exhibited significant co-regulation following BG intervention (**Fig S4A**). And differential gene expression of genes within this module was most significant on day 7 post-DSS treatment when comparing the BG-treated mice to PBS controls (**Fig S4B**). GO analysis revealed significant enrichment in pathways related to chemotaxis and leukocyte migration (**Fig 2A**). KEGG pathway enrichment analysis demonstrated significant activation of cellular processes involved in phagocytic function (**Fig 2B**) Additionally, the enrichment observed in WGCNA was further corroborated by whole-genome analysis of day 7 colitis samples, which also identified significant enrichment of pathways associated with chemotaxis, leukocyte migration and phagocytic function (**Fig S4C and S4D**). Multiple analytical approaches concurrently indicated that BG pretreatment not only enhances the recruitment of immune cells but also promotes their functional activation, particularly with respect to phagocytic capabilities.

To further investigate how BG pretreatment reprograms of intestinal myeloid cells, we performed single-cell RNA-seq to characterize intestinal leukocytes populations on day 7 post-DSS treatment. Unbiased clustering analysis identified multiple clusters of intestinal immune cells subsets, including monocytes/macrophages (*Ly6c2*, *Ccr2* and *Adgre1*), dendritic (DC) (*Cst3* and *H2-Aa*), neutrophils (*S100a8/a9* and *Ly6g*), B (*Cd79a Cd79b* and *Cd19*), Pre B (*Myl4* and *Mme*), CD4 T (*Cd3d* and *Cd4*), CD8 T (*Cd3d* and *Cd8a*), natural killer (*Nkg7*), ILC2 (*Gata3* and *Il4*) and ILC3 (*Rorc* and *Il22*) cells (**Fig 2C and Fig S4E**). Importantly, the ratio of monocytes/macrophages and neutrophils was elevated in the BG group (**Fig 2D**).

Single-cell RNA-sequencing data further demonstrated enhanced expression of innate pathogen

recognition receptors (*Syk*, *Nod1*, *Nod2*, *Tlr2* and *Tlr4*), efferocytosis (*Cd300lf*, *Axl*, *Mertk*, *Itgal* and *Itgb7*), cytokines (*Il1b*, *Il1rn*, *Vegfa* and *Tgfb1*), chemokines (*Ccl2*, *Ccl6*, *Ccl9*, *Cxcl9*) and chemokine receptors (*Ccr1*, *Ccr2*, *Cxcr4*) in intestinal monocytes/macrophages (**Fig 2E**). AUC and KEGG analysis demonstrated significant enrichment pathways related to activation of innate immune response and phagocytosis in monocytes/macrophages from BG-treated mice (**Fig 2F and 2G**). These findings, corroborated by WGCNA analysis, strongly suggest that BG pretreatment enhanced the recruitment and activation of myeloid cells, particularly monocytes/macrophages, in the inflamed colon, thereby improving disease outcomes.

BG trained bone marrow monocytes protected against colitis via the Ccl2-Ccr2 axis

Drawing upon single-cell transcriptome analysis that reveals the proportional expansion and functional reprogramming features of colonic monocyte/macrophage populations, in conjunction with the observation of significantly upregulated peripheral monocytes following BG pretreatment as depicted in **Fig S2B**. A hypothesis was formulated that BG exerts protective effects against colitis via monocytes. To experimentally validate this hypothesis, we evaluated the role of monocytes in *Ccr2* KO mice. Circulating Ly6C^{hi} monocytes were diminished in *Ccr2*$^{-/-}$ mice (**Fig S5A and S5B**), corroborating the pivotal role of the Ccl2-Ccr2 axis in monocyte egression from the bone marrow into circulation(19, 20). Notably, BG pretreatment failed to protect *Ccr2*$^{-/-}$ mice from DSS-induced colitis, as evidenced by the lack of significant differences in body weight loss, colon length, and epithelial permeability (**Fig 3A-E**).

In view of the fact that BG induces myelopoiesis through the modulation of hematopoietic stem and progenitors cell compartments in the bone marrow via central trained immunity(21, 22). we assessed whether transplantation of bone marrow cells from BG-pretreated donors could confer resistance to DSS-induced colitis in naïve recipients (**Fig 3F**). At 6 weeks post-transplantation, circulating myeloid cells were predominately derived from donor mice as indicated by the CD45.1 marker on circulating mononuclear cells (**Fig S5C**). Following DSS treatment, mice receiving bone marrow cells from BG-pretreated donors exhibited significantly reduced body weight loss

(**Fig 3G**). However, no significant difference in colon length was observed (**Fig 3H and Fig S5D**). Meanwhile, the percentage of circulating CD11b^{+} myeloid cells, neutrophils and Ly6C^{hi} monocytes were increased (**Fig 3I and J**, **Fig S5E**).

To further assess the role of monocyte, we adoptively transferred bone marrow Ly6C^{hi} monocytes sorted from control or BG-trained donor mice into *Ccr2*$^{-/-}$ recipient mice, which were then subjected to DSS treatment (**Fig S5F and S5G**). Mice received BG-trained monocytes exhibited reduced weight loss and colon shortening (**Fig 3K and 3L**). These findings suggest that BG-trained Ly6C^{hi} Ccr2^{+} monocytes play a pivotal role in the alleviation of colitis.

BG-trained monocytes enhance innate immune activation and microbial control

To explore the heterogeneity and functional roles of monocytes and macrophages, we delved deeper into the scRNA-seq data. By examining the expression of key signature genes, including *Ly6c2*, *Ccr2*, *H2-Ab1*, *Runx3*, *Itgax*, *Adgre1*, *Cx3cr1* and *Cd209a*, we identified eight distinct immune cell subsets: three monocyte subsets (Mono1-3) characterized by high *Ly6c2* and *Ccr2* expression, four macrophage subsets (Macro1-4) defined by expression of *H2-Ab1*, *Runx3*, *Itgax*, *Adgre1*, and *Cx3cr1*, and a dendritic cell subset (Cd209a^{+}DC) expressing integrin *Itgax* and C-type lectin *CD209a* (**Fig 4A and Fig S6A**). Among macrophage subsets, Macro1 highly expressed *Vegfa*, suggesting that may be a mucosal repair-promoting macrophage population. Macro2 was enriched with tissue-resident macrophage signature genes (*Runx3*, *Dtx4*, *Cx3cr1*, *Hes1*). In contrast, Macro3 and Macro4 deviated from the main cluster in cell clustering analysis, showing significant heterogeneity. Macro3 was characterized by high *Ighm* expression, while Macro4 showed elevated *Cd4* expression. Both Macro2 and Macro4 exhibited higher *Il10* expression than other monocyte/macrophage subsets, indicating their inflammation-regulatory functions.

The BG-treated group exhibited a significant increase in the proportions of Mono1, Mono2, Macro1, and CD209a^{+}DCs, whereas higher proportions of Mono3 and Macro3 were observed in the PBS group (**Fig 4B**). Given the strong enrichment of Mono1 and the reduction of Mono3 following BG treatment, we sought to further define the transcriptomic characteristics that differentiate Mono1 from Mono3. GO enrichment analysis revealed that Mono1 was significantly enriched in pathways regulating the activation of innate immune response (**Fig S6B**). KEGG pathways analysis further identified enrichment in NOD-like receptor (NLR) signaling, Toll-like receptor (TLR) signaling, and phagocytosis (**Fig 4C**). AUC analysis further confirmed the TLR

and NLR signaling pathways were significantly upregulated in Mono1 and Mono2 subsets of the BG-pretreated group (**Fig S6C and S6D**). Additionally, antimicrobial humoral response pathway was also upregulated in these two subclusters (**Fig S6E**). Cooperative activation of the pattern recognition receptor (PRR) signaling axis and antimicrobial humoral response significantly promotes the synthesis of antimicrobial peptides(23, 24). BG pretreatment significantly upregulated genes encoding pattern recognition receptors (*Nod1*, *Nod2*, *Tlr2*, *Tlr4*) and antimicrobial effector molecules (*S100a8*, *S100a9*, *Lcn2* and *Defb1*) in the colon on day 7 of colitis (**Fig 4D**). Furthermore, antimicrobial genes *S100a8* and *Defa1* were highly expressed in the BG group as validated by qPCR analysis (**Fig S6F**). These genes upregulation suggest a potential link between trained immunity and enhanced microbial control. Consistently, gene signatures associated with bacterial defense responses were prominently enriched in the BG-treated group (**Fig 4E**).

Previous studies have demonstrated that GBPs as intracellular effectors induced by IFNγ and LPS to promote antibacterial defense(25, 26). We found that BG training significantly enriched the IFN-γ response pathway in Mono1 and Mono2 subsets (**Fig S6G**). Meanwhile, Guanylate-binding proteins (GBP)-related genes, including *Gbp2*, *Gbp3*, *Gbp5*, and *Gbp7*, were also specifically upregulated in Mono1 and Mono2 (**Fig 4F**). GBP-deficient mice exhibit significantly increased susceptibility to *Salmonella typhimurium* infection(27-29). We then performed intestinal *Salmonella typhimurium* infection to assess whether BG pretreatment enhances microbial control in the gut (**Fig 4G**). As expected, BG pretreatment significantly protected mice from lethal *Salmonella Typhimurium* infection, suggesting that BG-induced trained immunity enhances mucosal defenses against gut microbial infections (**Fig 4H**).

Taken together, these results reinforced our bulk RNA-seq findings, indicating that BG pretreatment induces a specific monocyte subcluster with enhanced innate activation and phagocytic capacity, facilitating more efficient control of the breaching microbiome associated with DSS-induced leaky gut.

BG-mediated reprogramming of myeloid differentiation trajectories balances

inflammation and enhances mucosal repair in colitis

While BG-induced trained immunity is characterized by enhanced pro-inflammatory cytokine production and increased bactericidal capacity(14), excessive pro-inflammatory cytokines release may exacerbate colitis progression. To balance heightened cytokine production without inducing overwhelming immunopathology, we hypothesized that BG pretreatment might involve feedback loops that modulate the inflammation while preserving enhanced phagocytic capacity.

To investigate this, we analyzed previously obtained bulk colonic RNA-seq data, focusing on genes associated with anti-inflammatory and regulatory functions. On day 7 of colitis, BG pretreatment significantly upregulated genes encoding immunomodulatory factors (*Il4*, *Il10*, *Il11* and *Il33*), signaling inhibitors (*Socs1*, *Socs3*), and differentiation regulators (*Csf1*, *Csf1r*, *Stat3* and *Stat6*) (**Fig S7A**) The upregulation of *Socs1* and *Socs3* was further corroborated by scRNA-seq data, which showed increased expression of these genes in the Mono1 and Mono2 subclusters (**Fig S7B**). As members of the suppressor of cytokine signaling (SOCS) family, SOCS1 and SOCS3 inhibit excessive JAK-STAT signaling activation via negative feedback regulation(30-32). Moreover, coordinated activation of the monocyte/macrophage differentiation regulatory network (*Csf1r*, *Nr4a2*, *Irf8*, *Klf4*) suggests that BG may induce the differentiation of regulatory-phenotype macrophage subsets by reprogramming myeloid developmental trajectories, thereby modulating inflammatory responses.

To further investigate whether BG pretreatment reprograms monocyte-to-macrophage differentiation, we analyzed the day7 RNA-seq data revealed significant enrichment of myeloid leukocyte differentiation pathway (**Fig S7C**). Additionally, Single-cell trajectory analysis further revealed that Macro1 and Macro2 differentiated from Mono2 and Mono3, respectively (**Fig 5A**). BG training significantly accelerated the differentiation kinetics of Mono3 into Macro1, which may underlie the reduced frequency of the Mono3 subset in the BG group. Coupled with the gene expression signatures in **Fig S6A**, Macro1 shares similarities with Macro2 in marker gene expression, and the differentiated Macro1 subset could further differentiate into the tissue-resident macrophage Macro2 subset (**Fig 5B**).

Furthermore, we observed that the expression levels of *Ccr2* and *Ly6c2* decreased from Mono1 to Macro2, while *H2-Ab1* and *Cx3cr1* progressively increased, particularly in macrophages (**Fig 5C**). Since Cx3cr1 upregulation is a hallmark of circulating monocytes migrating to the intestinal lamina propria and undergoing macrophage differentiation(33), we used *CX3CR1-GFP* reporter mice to monitor the monocyte-to-macrophage transition in the DSS colitis model. In circulating leukocyte subsets, the total percentage of $CD11b^+$ myeloid cells was higher in BG-pretreated mice compared to controls (**Fig S8A-C**). A similar trend was observed in neutrophils (**Fig S8D and S8E**). While the initial monocyte percentage was higher in the BG group, no significant difference was observed the two groups on day 7 post-DSS treatment (**Fig 5D and S8F**), suggesting that circulating monocytes in BG-pretreated mice had extravasated into the intestinal tissue. Meanwhile, the percentage of colonic $CD11b^+$ myeloid cells and neutrophils was increased in the BG-pretreated group (**Fig S9A-C**).

We further defined monocyte/macrophage populations from P1 to P6 based on the expression of CD11b, CX3CR1-GFP, Ly6C, and MHCII. P1 to P3 were gated from $CD11b^+$&$CX3CR1\text{-}GFP^-$&$Ly6G^-$ cells. While P1 ($Ly6C^+$&$MHCII^-$) and P3 ($Ly6C^-$&$MHCII^+$) were comparable between group, P2 ($Ly6C^+$&$MHCII^+$) was increased in BG-pretreated mice (**Fig 5E**). P4 to P6 are gating from $CD11b^+$&$CX3CR1\text{-}GFP^+$ cells and further separate by the expression of Ly6C and MHCII. P4 ($Ly6C^+$&$MHCII^-$) as infiltrating monocytes gaining CX3CR1 expression. P5 ($Ly6C^+$&$MHCII^+$) is regarded as intermediate transitory immature macrophage and P6 ($Ly6C^-$&$MHCII^+$) is considered as mature macrophage as it completely loss expression of Ly6C and highly express MHCII. BG pretreatment led to an increase in P5 level (**Fig 5F**). The increase of P2 and P5 in BG group in line with the decrease of monocytes at day 7 in circulation post DSS treatment, suggesting that BG trained monocytes have higher capacity to infiltrate into the damaged colon and undergo macrophage differentiation.

Previous WGCNA analysis suggested that BG pre-treatment upregulated the focal adhesion pathway, which may enhance tissue repair mechanisms (**Fig 2B**). Consistent with this, we observed increased expression of genes involved in wound healing and tissue repair, such as

Mmp-related genes, *Spon1*, *Notch1*, *Notch2*, *Tgfb*, *Fgf1*, *Fgf2*, *Col1a1*, *Col1a2*, *and Fn1* in the BG-treated group on day 7, followed by a rapid decline by day 12. In contrast, the PBS group exhibited a much milder induction of these genes, with several genes remaining at comparable levels between day 7 and day 12 (**Fig 5G**). This led us to hypothesize that the upregulated monocytes and macrophages in the BG-treated group might exhibit enhanced expression of tissue repair-associated genes. As expected, the expression of *Spon1* and *Mmp14*, which promote the mucosal repair was increased in Mono2, Macro1, and Macro2 (**Fig 5H and 5I**). These findings suggest that BG pretreatment indeed induced monocyte and macrophage subsets with enhanced tissue repair capacity.

Discussion

Trained immunity, a non-antigen-specific form of innate immunological memory, enables rapid host defense mobilization upon pathogen challenge(34, 35). In inflammatory bowel disease, gut microbial dysbiosis manifests as reduced α-diversity, diminished commensal taxa (e.g., *Faecalibacterium prausnitzii*), and pathobiont expansion (e.g., *Enterobacteriaceae*, *adherent-invasive Escherichia coli*), which may compromise intestinal barrier integrity and precipitate microbial translocation(36-38). Additionally, the long-term use of immunosuppressants and biologics in IBD patients elevates infection susceptibility, rendering the microbial-controlling properties of trained immunity a viable therapeutic strategy for IBD(39). However, Excessive or sustained immune activation could trigger chronic inflammatory cascades and provoke autoimmune tissue damage through aberrant immune recognition, such as rheumatoid arthritis and cardiovascular diseases(9, 40-42). However, the functional correlation between trained immunity and colitis remains unclear, and how to apply trained immunity to colitis treatment represents an urgently unresolved scientific question.

Here, we demonstrated that BG-induced trained immunity confers cross-pathogen protective effects using a lethal *Staphylococcus aureus* infection model, while failing to induce intestinal inflammation under conditions of an intact mucosal barrier. Further investigations revealed that BG effectively attenuated dextran sulfate sodium (DSS)-induced colitis upon secondary challenge. BG pretreatment conferred long-term protection against DSS-induced colitis, with benefits lasting for at least two months after the peripheral myeloid cell populations returned to baseline levels. Bone marrow transplantation experiments confirmed that BG-induced trained immunity persists within hematopoietic progenitors, leading to durable reprogramming of peripheral monocytes. This long-term effect is likely supported by epigenetic modifications in hematopoietic cells, as reported in previous studies(21, 43). These findings highlight the potential of BG-induced trained immunity in establishing long-lasting immune memory, which could be leveraged to achieve sustained therapeutic effects in IBD.

The conventional understanding of IBD pathogenesis has long posited that abnormal immune activation is central to disease development and progression. This paradigm has predominantly focused on the role of adaptive immunity, particularly the dysregulation of Th17 and Treg functions over the past decades(44-46). However, our results suggest that BG-induced protection

is independent of adaptive immune responses. Even in *Rag1*$^{-/-}$ mice, which lack adaptive immunity, BG pretreatment significantly improved DSS-induced colitis outcomes. This underscores the dominant role of innate immunity.

In DSS-induced colitis, epithelial barrier disruption facilitates microbiota translocation across the mucosal epithelium, triggering inflammatory responses mediated by innate cells(38, 47, 48). We identified monocytes as key mediators of BG-induced protection against DSS-induced colitis, as demonstrated by experiments using *Ccr2*$^{-/-}$ mouse models and monocyte transfer studies. BG pretreatment enriched Ly6C^{hi}CCR2^{+} monocytes, which exhibited enhanced antimicrobial capabilities, as revealed by scRNA-seq. Ly6C^{hi}CCR2^{+} monocytes displayed higher levels of antimicrobial receptors like NOD2, TLR4 and GBP-related gene. Guanylate-binding protein (GBP) enhances *Salmonella* clearance by promoting inflammasome activation and intracellular bacterial elimination, particularly through disrupting *Salmonella*-containing vacuoles and inducting pyroptosis(27, 49). Our finding revealed that BG pretreatment increased resistance to *Salmonella typhimurium* infection. As inflammation and infection is partially controlled, monocytes can differentiate into macrophage subsets with anti-inflammatory and tissue repair functions, secreting cytokines such as IL-10, TGF-β and VEGF to promote inflammation resolution and tissue repair(50, 51).

Previous studies have underscored the essential role of circulating Ly6C^{hi} monocytes in replenishing intestinal macrophages(52, 53). During colitis and infection, these monocytes are rapidly recruited to injured colonic tissues, where they differentiate into Cx3cr1^{+} macrophages. We also observed that these monocytes exhibited enhanced migratory capabilities, enabling them to infiltrate inflamed tissues and differentiate into CX3CR1^{+} macrophages. These macrophages contribute to mucosal repair by clearing pathogens such as *Salmonella* and promoting epithelial regeneration(54). Single-cell trajectory analysis further showed that BG training promoted the differentiation of Macro1 into Macro2, which is consistent with the dynamic process of monocyte-to-mature macrophage conversion observed in *CX3CR1-GFP* reporter mice. Maintaining a balance between inflammatory monocytes, differentiated macrophages, and

tissue-resident macrophages is critical for resolving inflammation, promoting tissue repair(33, 55). These findings suggest that BG not only augments monocyte antimicrobial functions but also facilitates their differentiation into macrophages, enhancing their ability to recognize, phagocytose, and eliminate bacteria while promoting tissue repair. This dual function likely strengthens the intestinal barrier, mitigates inflammation, and supports gut homeostasis.

In the clinical exploration of IBD treatment, novel therapies based on cellular regeneration (intestinal organoid transplantation) and fecal microbiota transplantation (FMT) are emerging as critical avenues to overcome the limitations of conventional pharmacotherapies(56-58). Given the efficacy of BG-induced trained immunity in alleviating DSS-induced colitis, this approach holds significant promise as a novel therapeutic strategy for IBD treatment. We transferred BG-preconditioned monocytes significantly alleviated clinical symptoms, including weight loss and colon shortening, demonstrating the potential of cell-based therapies (**Fig S10A-C**).

In conclusion, BG confers long-term colitis amelioration through trained immunity by reprogramming bone marrow-derived monocytes. Mechanistically, BG enhances monocyte chemotaxis and antimicrobial functionality activation, enabling efficient microbial containment. Crucially, this trained state establishes self-regulating circuits, engaging in negative feedback regulation of excessive immune responses, while accelerated $CX3CR1^{+}$ macrophage differentiation facilitates mucosal repair. These findings establish a foundation for leveraging trained immunity as a therapeutic strategy for IBD, highlighting the potential of BG in modulating intestinal immunity and restoring gut homeostasis.

Materials and Methods

Animals

C57BL/6J wild-type male mice (6-8weeks) were purchased from Xiamen University Laboratory Animal Center. *Rag1*$^{-/-}$ and *CX3CR1-GFP* mice were generously provided by Dr. Kairui Mao and Dr.Xiaofen Chen from Xiamen University, respectively. *Ccr2*$^{-/-}$ mice were kindly provided by Dr. Shih-Chin Cheng from Xiamen University. Mice were maintained under specific pathogen-free conditions. All animal protocols were reviewed and approved by the Institutional Animal Care and Use Committee of Xiamen University.

In vivo beta-glucan (BG) training and DSS colitis model

Mice were i.p. injected with one dose of BG (1 mg) on day -7/-49, Then, Mice received 3% indicated DSS (36,000 to 50,000 molecular weight; MP Biomedicals) in their drinking water for 5 days, followed by 2 days or 7 days of distilled water without DSS. Control animals received distilled water for the entire period. Mice were monitored every day from day 0 for body weight until day 7 or 12.

Histology

Colons were collected from sacrificed mice at the end of each treatment schedule, as described above, colon was fixed with 4% paraformaldehyde and embedded in Paraffin. Tissue sections (5 μm) were prepared, deparaffinized, and stained with hematoxylin and eosin. with minor modifications, by assessing mucosa thickening, inflammatory cells, and submucosa cell infiltration. Each criterion was scored as 0-4, and the sum of each score was defined as the histological score. Histological scores were assigned by experimenters “blinded” to sample identity.

Coloscopy

A coloscopy system (ENDOCAM® Logic HD, RICHARD WOLF) was used to monitor the severity of DSS-induced colitis. After an 8-hour fast, we administered isoflurane (RWD, Co. Ltd.) and applied glycerin to the anus for smooth insertion.

In vivo intestine permeability assay

Age and sex-matched mice were orally administered with 0.6 mg/g body weight of an 100 mg/ml solution of FITC-dextran (FD4, Sigma). 5 hours later, retro-orbital blood was collected from each mouse. Serum was prepared by allowing the blood to clot by leaving it undisturbed overnight at 4°C and then subsequently centrifuged at 5000 rpm for 10 minutes. Dilutions of FITC-dextran in PBS and separately in pooled mouse serum were used as a standard curve. Absorbance of 50 µl serum was measured at microplate reader with excitation and emission filters set at 490 and 530 nm, respectively. Experiments were performed at least two independent times each in triplicate.

RNA extraction and real-time PCR

Total RNA was extracted from colon tissue previously washed from luminal content. Samples were homogenized in TRIZOL. Homogenized tissues were then added with chloroform in order to separate RNA from genomic DNA and proteins. RNA isolation and purification required isopropanol (RNA precipitation) and 70% ethanol (RNA wash). Total RNA was resuspended in Nuclease-free water. Subsequently, 1 µg of RNA was reverse-transcribed using the Hifair® ll lst Strand cDNA Synthesis SuperMix for qPCR (gDNA digester plus) following manufacturer's instructions. cDNA analysed through quantitative Real-Time PCR.

Isolation of cells from lamina propria

To isolate lamina propria mononuclear cells (lamina propria MCs), extraintestinal fat tissue was carefully removed and colons were then flushed of their luminal content with physiologic solution, opened longitudinally and cut into 1 cm pieces. Epithelial cells and mucus were removed by incubation with 10 mL of D-Hank's balanced salt solution (containing EDTA and DTT, free of $Ca2^{+}$ and $Mg2^{+}$) for 20 minutes at 37°C at 200 rpm in a constant temperature shaker. Colon pieces were then digested in Hank's (with $Ca2^{+}$ and $Mg2^{+}$) containing 0.5 mg/ml Collagenase IV and 15 µg/ml DNase I, for 40 min at 37°C shaking at 200 rpm. The remaining cells were centrifuged and resuspended in FACS buffer (1% FBS, 2 mM EDTA in PBS).

Bone Marrow Transplantation

Wild type CD45.2 mice were subjected to 8 Gy irradiation (RAD SOURCE, RS2000). CD45.1 wild type and BG trained mice were sacrificed, and the femurs were used to harvest bone marrow cells. 1×10^7 bone marrow cells from CD45.1 wild type and BG trained donor mice were transferred to irradiated CD45.2 recipients via tail-vein injection. 2.5% DSS was given at 6 weeks-post bone marrow transplantation. Mice were monitored every day until day 12.

Adoptive transfer of bone marrow monocytes

BG trained mice were sacrificed, and the femurs were used to harvest bone marrow cells, Bone marrow cells were stained with the following panel: Biotin antibody (B220, CD4, CD8, NK1.1, Ly6G), Live/dead (Cat. L34976, Invitrogen), CD45 (Cat. 45-0451-82, Clone. 30-F11, ebioscience), CD11b (Cat. 48-0112-82, Clone. M1/70, ebioscience), Ly6C (Cat. 128016, Clone. HK1.4, Biolegend). Biotin-labeled lineage antibodies were used to stain bone marrow cells at 4℃ for 20 min and then incubated with fluorescence conjugated streptomycin together with other surface protein antibodies for another 20 min. $Ly6C^{hi}$ monocytes were sorted to > 97% purity using a BD Aria III cell sorter.

RNA-seq

RNA was extracted from colon LPLs of individual mice. RNA integrity was assessed using the RNA Nano 6000 Assay Kit of the Bioanalyzer 2100 system (Agilent Technologies, CA, USA). The clustering of the index-coded samples was performed on a cBot Cluster Generation System using TruSeq PE Cluster Kit v3-cBot-HS (Illumia) according to the manufacturer's instructions. The library was sequenced on an Illumina Novaseq platform and 150 bp paired-end reads were generated.

scRNA-seq

Isolated lamina propria mononuclear cells, sample from three mice were pooled together and analyzed per condition. For scRNA-seq of Colon $CD45^+$ cells were sorted by BD Arial III. These cells were barcoded with 10× Cellplex oligos before being encapsulated using the 10X Chromium 3′ Reagent Kits v3 according to manufacturer's instructions.

RNA-seq data processing and analysis

Raw data of fastq format were quality checked through fastqc software. Reference genome and gene model annotation files were downloaded from genome (mm10) website directly. Index of the reference genome was built using Hisat2 v2.1.0 and paired-end clean reads were aligned to the reference genome using Hisat2 v2.1.0. Expression levels across the sample were expressed in FPKM (Fragment per kilobase per million). Weighted correlation network analysis was perform using an R package from horvath.genetics.ucla.edu/html/CoexpressionNetwork/Rpackages/WGCNA/. Differential gene expression was used DESeq2 by a twofold cutoff and pvalue < 0.05. All differentially expressed genes were plotted with the “pheatmap” and “ggplot2” R packages. For KEGG enrichment analysis, p-value < 0.05 was used as a threshold to determine significant enrichment for gene sets with the “clusterProfiler” R package.

scRNA-seq data processing and analysis

Raw sequencing data was processed and aligned mm10 mouse reference genome with CellRanger (10× Genomics) v 7.2.0. Resulting filtrated matrices (count matrices) of molecular counts were used as input for further processing with Seurat package V5.0.1running under R studio. First, quality control was performed to create Seurat object with min features > 200 and removal of cells having < 200 or > 8000 expressed genes or > 5% mitochondrial counts. The total number of recovered cells was mentioned before. Variable features using FindVariableFeatures (using RNA and vst as an assay and selection method as parameters) and normalization using normalization.method = "LogNormalize", scale.factor = 10000 were performed . This integrated data is scaled using ScaleData function using all genes and “RNA” as assay method.

Doublet cells were filtered by DoubletFinder v3. Principal Component Analysis was performed on variable features using RunPCA and first 30 PCs were chosen. The nearest neighbors using the FindNeighbors(dims=1:12) and FindClusters(resolution=0.8) function. For visualization, the non-linear dimensional reduction such as UMAP analysis was using RunUMAP function from Seurat. To calculate pseudotime based on the Mono/Marco subset data using the monocle3.

Statistical Analysis

Statistical analyses were conducted using GraphPad Prism version 9.0 and R statistical software (version 4.2.2, R Foundation for Statistical Computing). Data were analyzed using a two-tailed Student's *t*-test. Multiple-group comparisons were performed using one-way or two-way analysis of variance (ANOVA) followed by Tukey's multiple-comparisons test. Survival data were assessed using Kaplan-Meier survival plots, followed by the log-rank test. Significant differences were indicated by an asterisk ($p < 0.05$).

Acknowledgments:

We thank the staff of Xiamen University Laboratory Animal Center. Special thank to Prof. Kairui Mao and Prof. Xiao-fen Chen for generously providing mice. We appreciate the help of Dr. Jia Zhang and other staff from Prof. Shih-Chin Cheng's laboratory during the study.

Author contributions:

Y.Y.L. designed and did the experiments, analyzed the data and wrote the paper; Y.Y.F., Q.X.G. and Q.Y. C. analyzed the data, wrote the paper, and supervised the study. Y.Q.H., L.W., H.X.S., E.M.C., Q.Y.X., Y.C., Q.Q.F., L.L.L provided advice and oversaw a portion of the work. J.L.R., S.-C.C., H.Z.X. conceived the idea, secured funding, supervised the study, helped in data interpretations, revised drafts of manuscript; supervised overall project. All authors reviewed and approved the final version of the manuscript.

Ethics statements

Patient consent for publication: Not applicable.

Ethics approval

All animal protocols were reviewed and approved by the Institutional Animal Care and Use Committee of Xiamen University.

Funding:

This project was supported by National Key R&D Program of China (2022YFA1304000),

National Natural Science Foundation of China (82300630&32161133020), Healthcare System Youth Backbone Talent Training Project of Fujian Province(2023GGB09), Municipal Natural Science Foundation of Xiamen (3502Z20227271), Foundation of State Key Laboratory of Vaccines for Infectious Diseases, Xiang An Biomedicine Laboratory (2023XAKJ0101012), Medical and Health Key Project of Xiamen (3502Z20204007).

Data availability statement

All data relevant to the study are included in the manuscript or uploaded as online supplemental information. Sequencing data have been deposited to the GEO with accession number GSE285859 (single cell RNA-seq), GSE285860 (RNA-seq).

Reference

1. Kobayashi T, Siegmund B, Le Berre C, Wei SC, Ferrante M, Shen B, et al. Ulcerative colitis. Nat Rev Dis Primers. 2020;6(1).
2. Dolinger M, Torres J, Vermeire S. Crohn's disease. Lancet. 2024;403(10432):1177-91.
3. Zhang F, Aschenbrenner D, Yoo JY, Zuo T. The gut mycobiome in health, disease, and clinical applications in association with the gut bacterial microbiome assembly. Lancet Microbe. 2022;3(12):E969-E83.
4. Abraham C, Medzhitov R. Interactions Between the Host Innate Immune System and Microbes in Inflammatory Bowel Disease. Gastroenterology. 2011;140(6):1729-37.
5. Jostins L, Ripke S, Weersma RK, Duerr RH, McGovern DP, Hui KY, et al. Host-microbe interactions have shaped the genetic architecture of inflammatory bowel disease. Nature. 2012;491(7422):119-24.
6. Wehkamp J, Harder J, Weichenthal M, Schwab M, Schäffeler E, Schlee M, et al. NOD2 (CARD15) mutations in Crohn's disease are associated with diminished mucosal α-defensin expression. Gut. 2004;53(11):1658-64.
7. Watanabe T, Kitani A, Murray PJ, Strober W. NOD2 is a negative regulator of Toll-like receptor 2-mediated T helper type 1 responses. Nat Immunol. 2004;5(8):800-8.
8. Noguchi E, Homma Y, Kang XY, Netea MG, Ma XJ. A Crohn's disease-associated NOD2 mutation suppresses transcription of human IL10 by inhibiting activity of the nuclear ribonucleoprotein hnRNP-A1. Nat Immunol. 2009;10(5):471-9.
9. Netea MG, Joosten LAB, Latz E, Mills KHG, Natoli G, Stunnenberg HG, et al. Trained immunity: A program of innate immune memory in health and disease. Science. 2016;352(6284).
10. Netea MG, Domínguez-Andrés J, Barreiro LB, Chavakis T, Divangahi M, Fuchs E, et al. Defining trained immunity and its role in health and disease. Nat Rev Immunol. 2020;20(6):375-88.
11. Ding CL, Shrestha R, Zhu XJ, Geller AE, Wu SZ, Woeste MR, et al. Inducing trained immunity in pro-metastatic macrophages to control tumor metastasis. Nat Immunol. 2023;24(2):239.

12. Jeyanathan M, Vaseghi-Shanjani M, Afkhami S, Grondin JA, Kang ALS, D'Agostino MR, et al. Parenteral BCG vaccine induces lung-resident memory macrophages and trained immunity via the gut-lung axis (vol 23, pg 1687, 2022). Nat Immunol. 2023;24(6):1049-.

13. Zhu YH, Gao QX, Zhang J, Cheng Y, Yang SZ, Xu R, et al. Persistent bone marrow hemozoin accumulation confers a survival advantage against bacterial infection via cell-intrinsic Myd88 signaling. Cell Rep. 2024;43(10).

14. Moorlag SJCFM, Khan N, Novakovic B, Kaufmann E, Jansen T, van Crevel R, et al. β-Glucan Induces Protective Trained Immunity against Mycobacterium tuberculosis Infection: A Key Role for IL-1. Cell Rep. 2020;31(7).

15. Cheng SC. mTOR- and HIF-1α-mediated aerobic glycolysis as metabolic basis for trained immunity (vol 346, aaa1503, 2014). Science. 2014;346(6211):821.

16. Kalafati L, Kourtzelis I, Schulte-Schrepping J, Li XF, Hatzioannou A, Grinenko T, et al. Innate Immune Training of Granulopoiesis Promotes Anti-tumor Activity. Cell. 2020;183(3):771.

17. Netea MG, Quintin J, van der Meer JWM. Trained Immunity: A Memory for Innate Host Defense. Cell Host Microbe. 2011;9(5):355-61.

18. Quintin J, Saeed S, Martens JHA, Giamarellos-Bourboulis EJ, Ifrim DC, Logie C, et al. Infection Affords Protection against Reinfection via Functional Reprogramming of Monocytes. Cell Host Microbe. 2012;12(2):223-32.

19. Tsou CL, Peters W, Si Y, Slaymaker S, Aslanian AM, Weisberg SP, et al. Critical roles for CCR2 and MCP-3 in monocyte mobilization from bone marrow and recruitment to inflammatory sites. J Clin Invest. 2007;117(4):902-9.

20. Geng HX, Chen LN, Tang J, Chen YA, Wang L. The Role of CCL2/CCR2 Axis in Cerebral Ischemia-Reperfusion Injury and Treatment: From Animal Experiments to Clinical Trials. Int J Mol Sci. 2022;23(7).

21. Mitroulis I, Ruppova K, Wang BM, Chen LS, Grzybek M, Grinenko T, et al. Modulation of Myelopoiesis Progenitors Is an Integral Component of Trained Immunity. Cell. 2018;172(1-2):147.

22. Chavakis T, Mitroulis I, Hajishengallis G. Hematopoietic progenitor cells as integrative hubs for adaptation to and fine-tuning of inflammation. Nat Immunol. 2019;20(7):802-11.

23. Muniz LR, Knosp C, Yeretssian G. Intestinal antimicrobial peptides during homeostasis, infection, and disease. Front Immunol. 2012;3.

24. Duarte-Mata DI, Salinas-Carmona MC. Antimicrobial peptides′ immune modulation role in intracellular bacterial infection. Front Immunol. 2023;14.

25. Sweet MJ, Ramnath D, Singhal A, Kapetanovic R. Inducible antibacterial responses in macrophages. Nat Rev Immunol. 2024.

26. Pilla DM, Hagar JA, Haldar AK, Mason AK, Degrandi D, Pfeffer K, et al. Guanylate binding proteins promote caspase-11-dependent pyroptosis in response to cytoplasmic LPS. P Natl Acad Sci USA. 2014;111(16):6046-51.

27. Man SM, Karki R, Sasai M, Place DE, Kesavardhana S, Temirov J, et al. IRGB10 Liberates Bacterial Ligands for Sensing by the AIM2 and Caspase-11-NLRP3 Inflammasomes. Cell. 2016;167(2):382.

28. Santos JC, Broz P. Sensing of invading pathogens by GBPs: At the crossroads between cell-autonomous and innate immunity. J Leukocyte Biol. 2018;104(4):729-35.

29. Meunier E, Dick MS, Dreier RF, Schürmann N, Broz DK, Warming S, et al. Caspase-11 activation requires lysis of pathogen-containing vacuoles by IFN-induced GTPases. Nature. 2014;509(7500):366.

30. Yuan FF, Peng W, Yang YY, Xu JQ, Liu YD, Xie Y, et al. Endothelial progenitor cell-derived exosomes promote anti-inflammatory macrophages via SOCS3/JAK2/STAT3 axis and improve the outcome of spinal cord injury. J Neuroinflamm. 2023;20(1).

31. Zhao YH, Peng F, He JY, Qu YL, Ni HM, Wu LL, et al. SOCS1 Peptidomimetic Alleviates Glomerular Inflammation in MsPGN by Inhibiting Macrophage M1 Polarization (vol 46, pg 2402, 2023). Inflammation. 2023;46(6).

32. Bidgood GM, Keating N, Doggett K, Nicholson SE. SOCS1 is a critical checkpoint in immune homeostasis, inflammation and tumor immunity. Front Immunol. 2024;15.

33. Li JY, Zhou HF, Fu XX, Zhang M, Sun F, Fan H. Dynamic role of macrophage CX3CR1 expression in inflammatory bowel disease. Immunol Lett. 2021;232:39-44.

34. Ziogas A, Bruno M, van der Meel R, Mulder WJM, Netea MG. Trained immunity: Target for prophylaxis and therapy. Cell Host Microbe. 2023;31(11):1776-91.

35. Ochando J, Mulder WJM, Madsen JC, Netea MG, Duivenvoorden R. Trained immunity - basic concepts and contributions to immunopathology. Nat Rev Nephrol. 2023;19(1):23-37.

36. Sauceda C, Bayne C, Sudqi K, Gonzalez A, Dulai PS, Knight R, et al. Stool multi-omics for the study of host-microbe interactions in inflammatory bowel disease. Gut Microbes. 2022;14(1).

37. Schaubeck M, Clavel T, Calasan J, Lagkouvardos I, Haange SB, Jehmlich N, et al. Dysbiotic gut microbiota causes transmissible Crohn's disease-like ileitis independent of failure in antimicrobial defence. Gut. 2016;65(2):225-37.

38. Palmela C, Chevarin C, Xu ZL, Torres J, Sevrin G, Hirten R, et al. Adherent-invasive Escherichia coli in inflammatory bowel disease. Gut. 2018;67(3):574-87.

39. Kirchgesner J, Lemaitre M, Carrat F, Zureik M, Carbonnel F, Dray-Spira R. Risk of Serious and Opportunistic Infections Associated With Treatment of Inflammatory Bowel Diseases. Gastroenterology. 2018;155(2):337.

40. Hu ZD, Lu SH, Lowrie DB, Fan XY. Trained immunity: A Yin-Yang balance. Medcomm. 2022;3(1).

41. Ospelt C, Reedquist KA, Gay S, Tak PP. Inflammatory memories: Is epigenetics the missing link to persistent stromal cell activation in rheumatoid arthritis? Autoimmun Rev. 2011;10(9):519-24.

42. Grigoriou M, Banos A, Filia A, Pavlidis P, Giannouli S, Karali V, et al. Transcriptome reprogramming and myeloid skewing in haematopoietic stem and progenitor cells in systemic lupus erythematosus. Ann Rheum Dis. 2020;79(2):242-53.

43. Tercan H, Riksen NP, Joosten LAB, Netea MG, Bekkering S. Trained Immunity: Long-Term Adaptation in Innate Immune Responses. Arterioscl Throm Vas. 2021;41(1):55-61.

44. Liu S, Cao YQ, Cui KR, Ren G, Zhao TT, Wang XZ, et al. Regulation of T helper cell differentiation by the interplay between histone modification and chromatin interaction. Immunity. 2024;57(5).

45. Kosinsky RL, Gonzalez MM, Saul D, Barros LL, Sagstetter MR, Fedyshyn Y, et al. The FOXP3^{+} Pro-Inflammatory T Cell: A Potential Therapeutic Target in Crohn's Disease. Gastroenterology. 2024;166(4).

46. Britton GJ, Contijoch EJ, Mogno I, Vennaro OH, Llewellyn SR, Ng R, et al. Microbiotas from Humans with Inflammatory Bowel Disease Alter the Balance of Gut Th17 and RORγt^{+} Regulatory T Cells and Exacerbate Colitis in Mice. Immunity. 2019;50(1):212.

47. Hernández-Chirlaque C, Aranda CJ, Ocón B, Capitán-Cañadas F, Ortega-González M, Carrero JJ, et al. Germ-free and Antibiotic-treated Mice are Highly Susceptible to Epithelial Injury in DSS Colitis. J Crohns Colitis. 2016;10(11):1324-35.

48. Panpetch W, Hiengrach P, Nilgate S, Tumwasorn S, Somboonna N, Wilantho A, et al. Additional *Candida albicans* administration enhances the severity of dextran sulfate solution induced colitis mouse model through leaky gut-enhanced systemic inflammation and gut-dysbiosis but attenuated by *Lactobacillus rhamnosus* L34. Gut Microbes. 2020;11(3):465-80.

49. Rupper AC, Cardelli JA. Induction of guanylate binding protein 5 by gamma interferon increases susceptibility to Salmonella enterica serovar Typhimurium-induced pyroptosis in RAW 264.7 cells. Infect Immun. 2008;76(6):2304-15.

50. Rigamonti A, Villar J, Segura E. Monocyte differentiation within tissues: a renewed outlook. Trends Immunol. 2023;44(12):999-1013.

51. Wynn TA, Vannella KM. Macrophages in Tissue Repair, Regeneration, and Fibrosis. Immunity. 2016;44(3):450-62.

52. De Schepper S, Verheijden S, Aguilera-Lizarraga J, Viola MF, Boesmans W, Stakenborg N, et al. Self-Maintaining Gut Macrophages Are Essential for Intestinal Homeostasis (vol 175, pg 400, 2018). Cell. 2019;176(3):676.

53. Bain CC, Scott CL, Uronen-Hansson H, Gudjonsson S, Jansson O, Grip O, et al. Resident and pro-inflammatory macrophages in the colon represent alternative context-dependent fates of the same Ly6Chi monocyte precursors. Mucosal Immunol. 2013;6(3):498-510.

54. Trebicka E, Shanmugam NKN, Chen KJ, Su CW, Shi HN, Cherayil BJ. Intestinal Inflammation Leads to a Long-lasting Increase in Resistance to Systemic Salmonellosis that Requires Macrophages

But Not B or T Lymphocytes at the Time of Pathogen Challenge. Inflamm Bowel Dis. 2015;21(12):2758-65.

55. Weber B, Saurer L, Schenk M, Dickgreber N, Mueller C. CX3CR1 defines functionally distinct intestinal mononuclear phagocyte subsets which maintain their respective functions during homeostatic and inflammatory conditions. Eur J Immunol. 2011;41(3):773-9.

56. Yui SR, Nakamura T, Sato T, Nemoto Y, Mizutani T, Zheng X, et al. Functional engraftment of colon epithelium expanded in vitro from a single adult Lgr5^{+} stem cell. Nat Med. 2012;18(4):618-23.

57. Lopetuso LR, Deleu S, Godny L, Petito V, Puca P, Facciotti F, et al. The first international Rome consensus conference on gut microbiota and faecal microbiota transplantation in inflammatory bowel disease. Gut. 2023;72(9):1642-50.

58. Haifer C, Luu LDW, Paramsothy S, Borody TJ, Leong RW, Kaakoush NO. Microbial determinants of effective donors in faecal microbiota transplantation for UC. Gut. 2023;72(1):90-100.

Fig 1. β-glucan (BG) pretreatment ameliorates DSS-induced colitis.

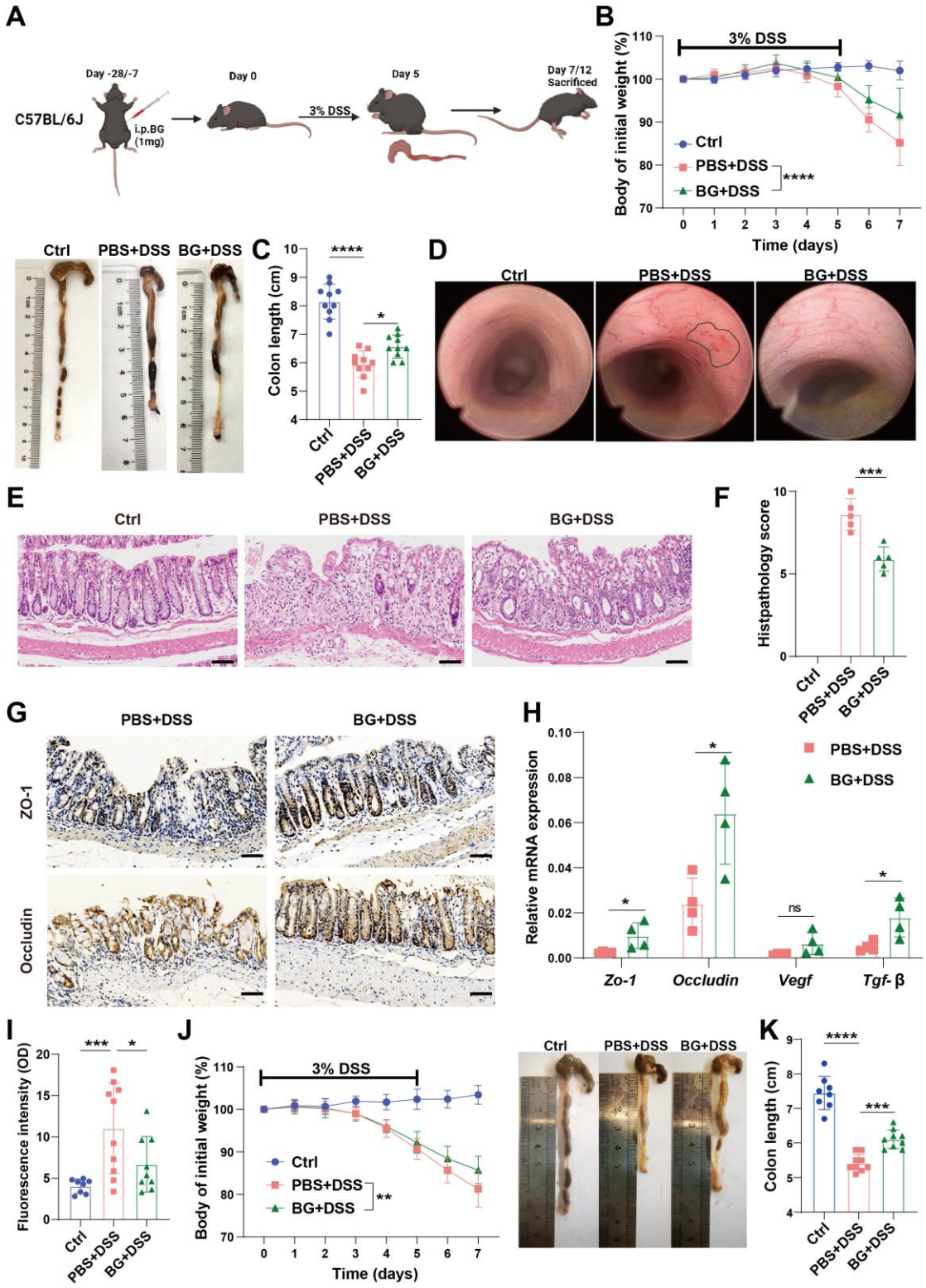

(A) Schematic representation of BG-induced trained immunity and DSS colitis model, (**B**) Body weight change curve of mice pretreated with BG for one week, followed by colitis induction with 3% DSS (n = 10), (**C**) Colon length changes in mice from (**B**), (**D**) Endoscopic images displaying mucosal damage, (**E and F**) H&E staining and histological scoring. Scale bars: 100 μm, (**G and H)** Expression levels of tight junction and repair, (**I**) FITC-dextran assay assessing intestinal barrier function, (**J**) Body weight change curve of mice pretreated with BG for four weeks, followed by colitis induction with 3% DSS (n = 8-9), (**K**) Colon length changes in mice from (**J**). Data are presented as mean ± SD. Statistical significance: *$p < 0.05$, **$p < 0.01$, ***$p < 0.001$, ****$p < 0.0001$. ns, not significant.

Fig 2. BG ameliorates colitis by enhancing myeloid cell activation.

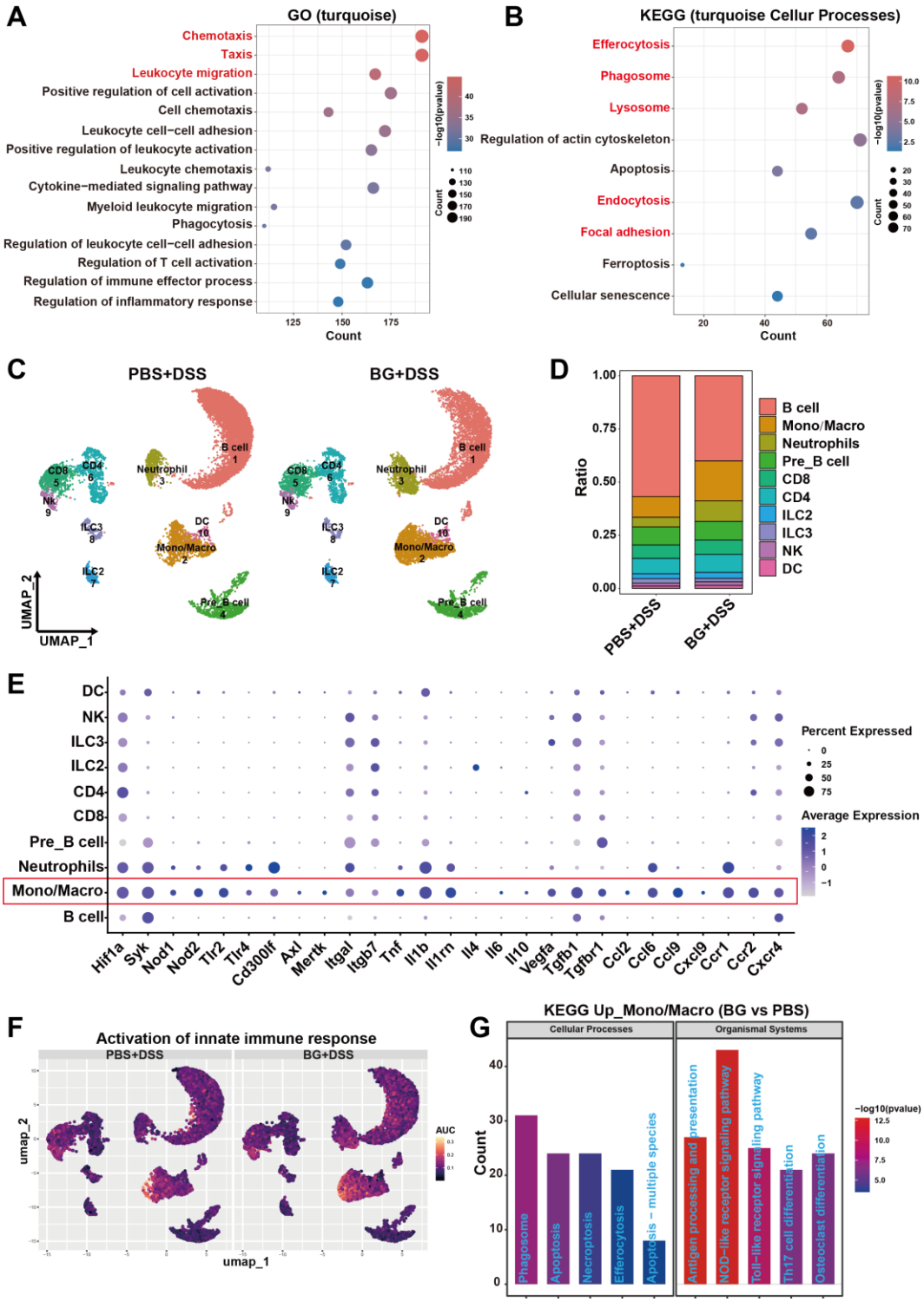

RNA sequencing of colon tissue at different time points of colitis. (**A**) GOBP and (**B**) KEGG pathway analyses of genes in the MEturquoise module. Single-cell RNA sequencing analysis of $CD45^+$ cells in the colon on day seven of colitis after one week of BG pretreatment. (**C**) UMAP plot of LP $CD45^+$ cells, (**D**) Cell ratio distribution from scRNA-seq data, (**E**) Dot plots showing representative DEGs between LP $CD45^+$ cells, (**F**) AUC scores for selected pathways, (**G**) KEGG pathway analysis of genes upregulated in the monocyte-macrophage lineage. DEGs, differentially expressed genes. LP, lamina propria. UMAP, uniform manifold approximation, and projection. AUC, area under the curve.

Fig 3. BG trained bone marrow monocytes protected against colitis via the Ccl2-Ccr2 axis.

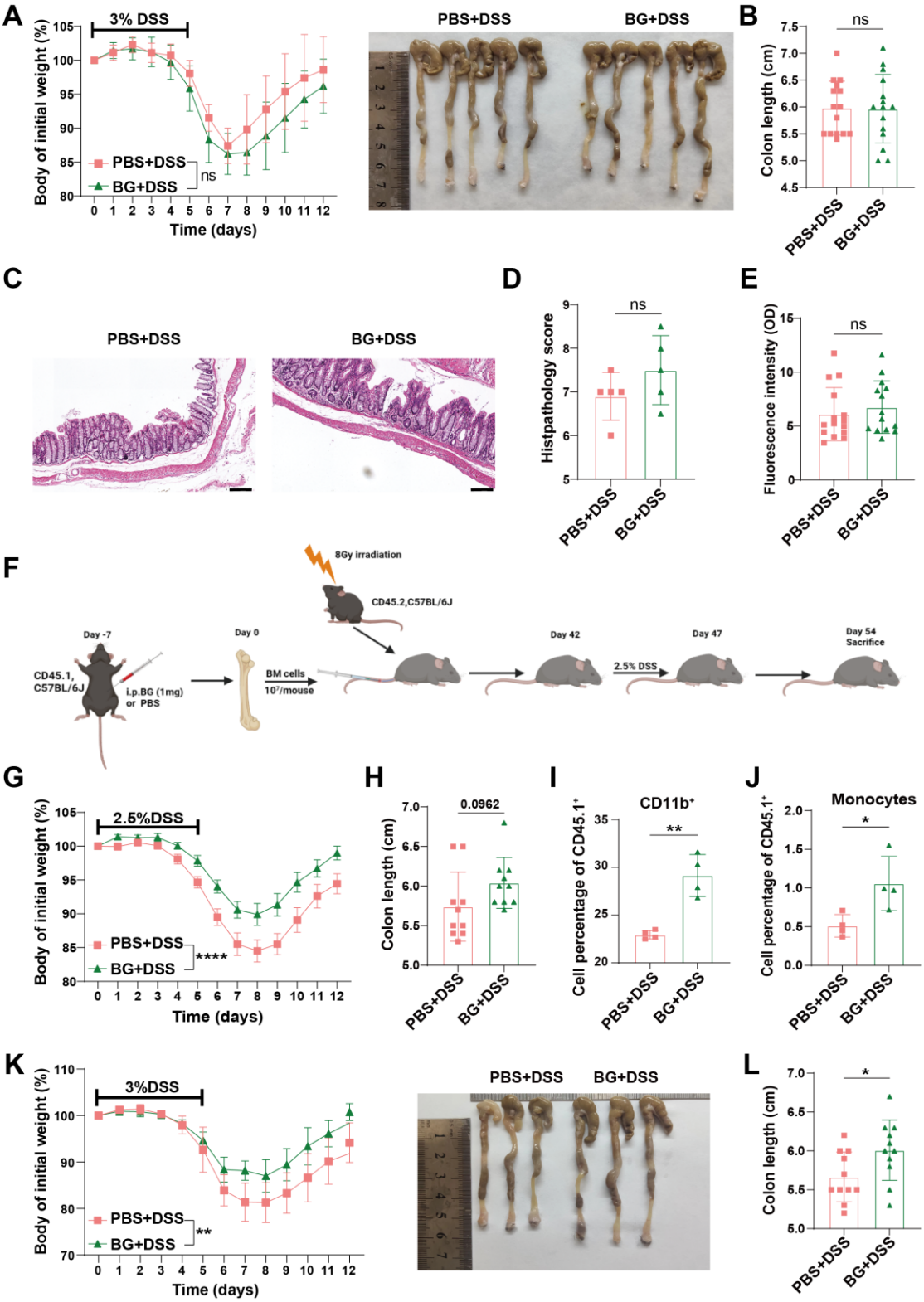

Ccr2$^{-/-}$ mice pretreated with BG for 1 week followed by induction of colitis with 3% DSS. (**A**) Changes in body weight (*n* = 15), (**B**) Colon length changes in *Ccr2*$^{-/-}$ mice from (**A**), (**C and D**) H&E staining and histological scoring, H&E. Scale bars: 100 μm, (**E**) FITC-dextran assay assessing intestinal barrier function, (**F**) Schematic representation of bone marrow transplantation from BG-pretreated CD45.1 mice to CD45.2 mice and colitis model, (**G**) Body weight change curve of colitis mice (*n* = 10), (**H**) Colon length changes in colitis mice from (**G**), (**I and J**)Percentage of CD11b^{+} (**I**) and Ly6C^{hi} monocytes (**J**) were analyzed by flow cytometry in peripheral blood, (**K and L**) Body weight change curve(**K**) and colon length changes of *Ccr2*$^{-/-}$ mice receiving Ly6C^{hi} monocyte adoptive transfer(**L**) (*n* = 11). Data are presented as mean ± SD. Statistical significance: **p* <0.05, ***p* <0.01, *****p* <0.0001. ns, not significant.

Fig 4. BG-trained monocytes enhance innate immune activation and microbial control.

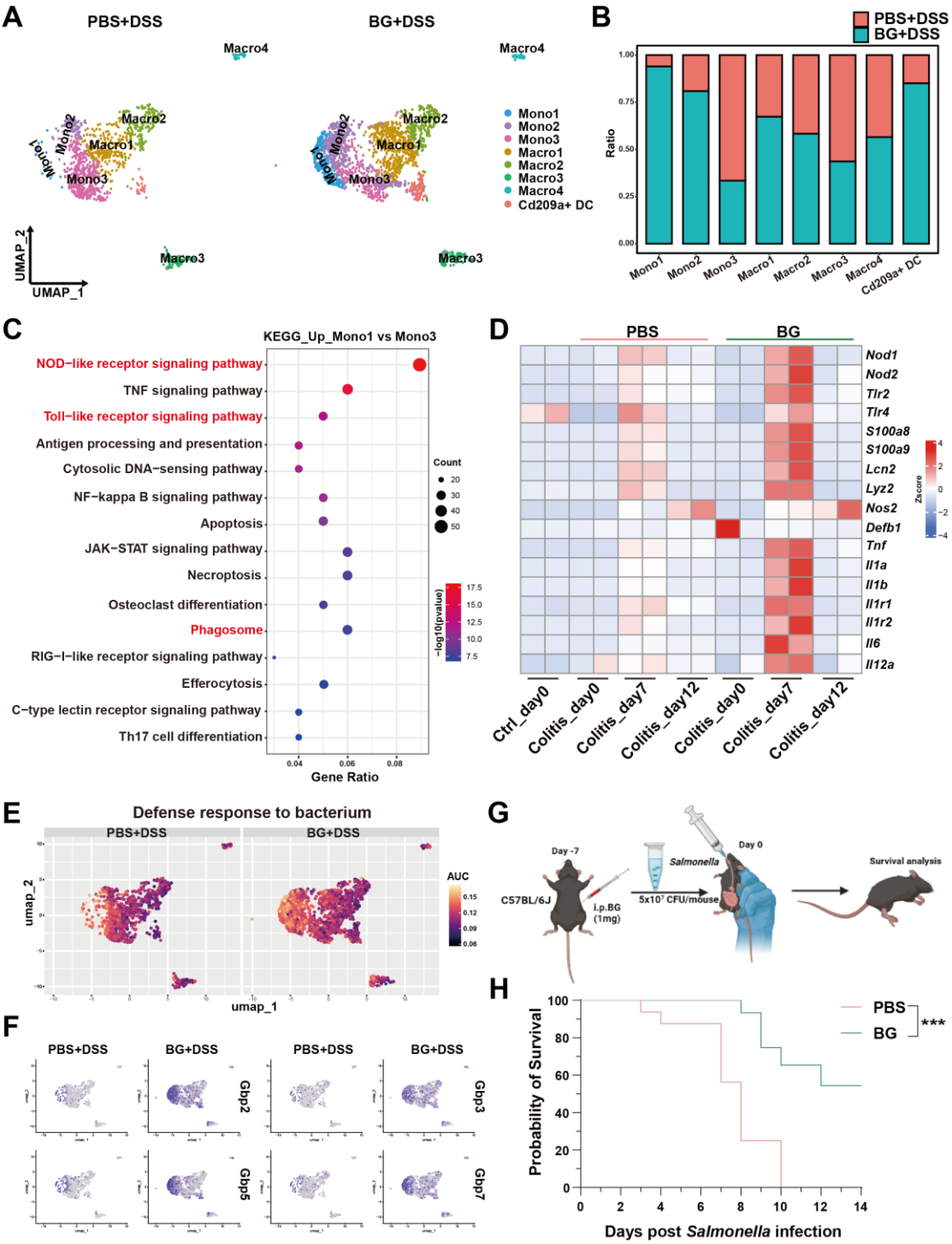

(**A**) UMAP and graphical visualization of the monocyte/macrophage lineage, (**B**) The ratio of monocyte/macrophage subsets, (**C**) KEGG pathway enrichment analysis of genes upregulated in monocyte 1 and monocyte 3, (**D**) Gene expression analysis at different time points of colitis, based on colon RNA sequencing, (**E**) AUC scores of selected pathways, (**F**) UMAP plots showing differential gene expression patterns, (**G**) Schematic representation *Salmonella* resistance after one week of BG pretreatment, (**H**) Survival curve of mice infected with *Salmonella* after one week of BG training. Statistical significance: ***$p < 0.001$.

Fig 5. BG-mediated reprogramming of myeloid differentiation trajectories balances inflammation and enhances mucosal repair in colitis.

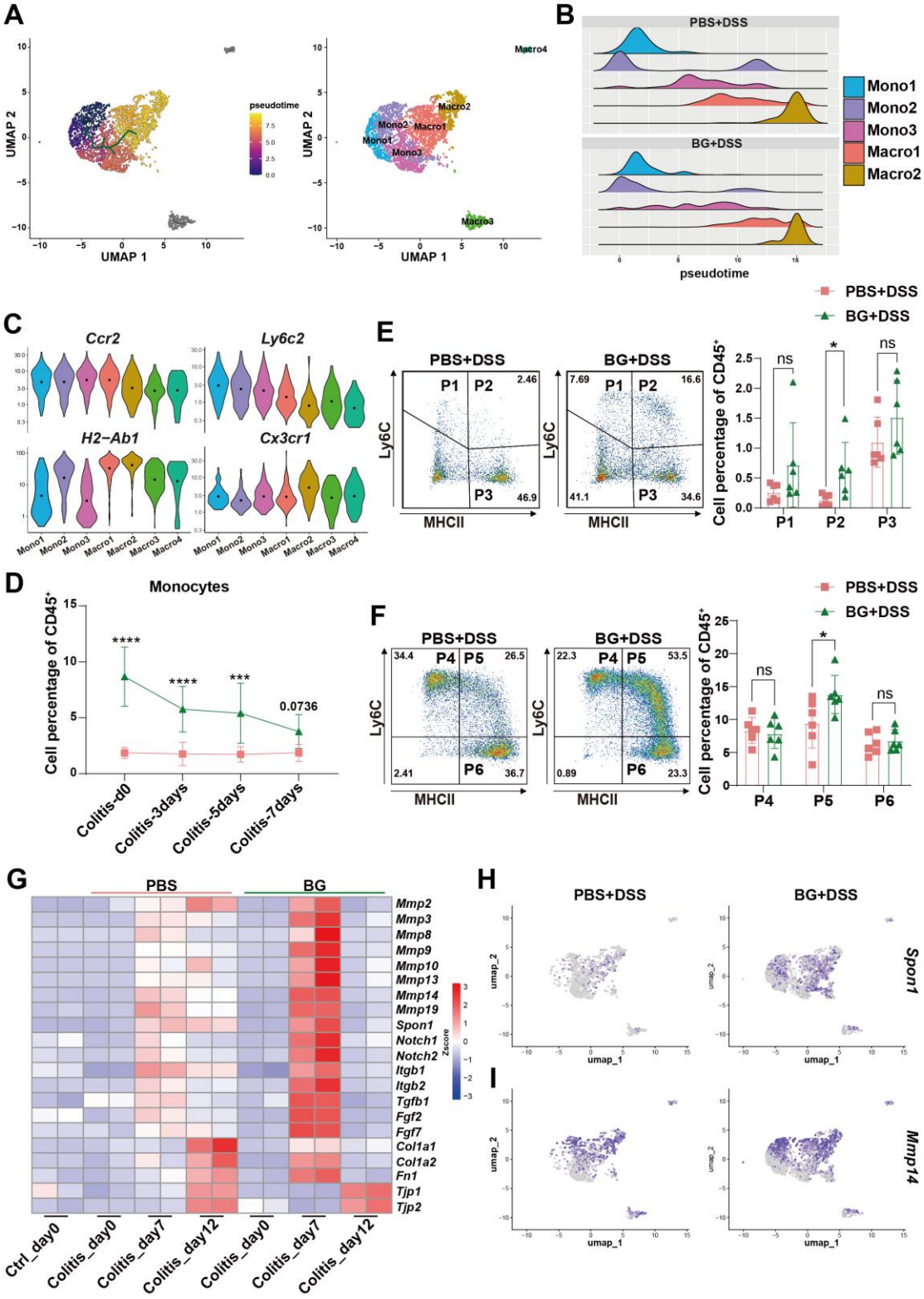

(**A**) Monocle 3 trajectory analysis of monocyte/macrophage subsets, (**B**) Ridgeline plot of monocyte/macrophage subsets, (**C**) Violin plots of surface marker gene expression in monocyte/macrophage subsets, (**D**) Percentage of monocytes in peripheral blood at different time points of colitis progression, (**E and F**) Colonic LPMCs were collected, and the percentages of monocyte/macrophage were analyzed on day 7 of colitis, (**G**) Expression of mucosal repair-related genes at different time points of colitis, (**H**) Gene expression analysis of the monocyte/macrophage lineage. Data are presented as mean ± SD. Statistical significance: *p <0.05, ***p <0.001; ****p <0.0001. ns, not significant.

Fig S1. BG pretreatment ameliorates DSS-induced colitis.

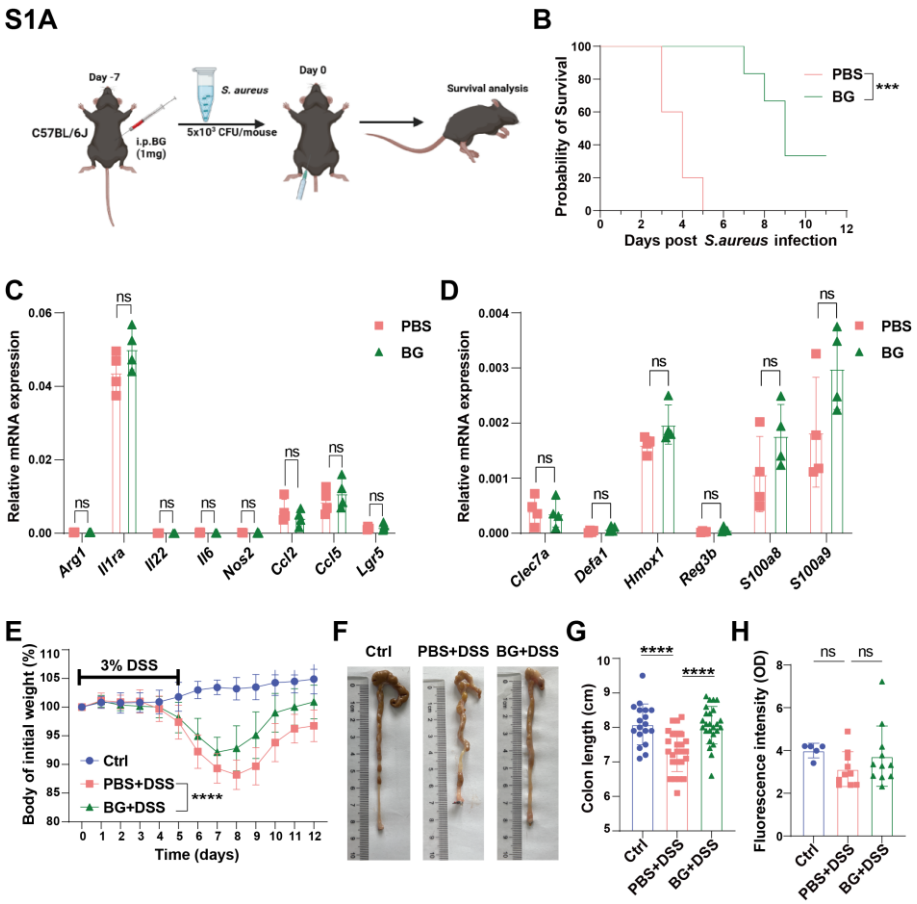

(**A**) Schematic representation of BG-induced trained immunity and *Staphylococcus aureus* infection model, (**B**) Survival curve of mice infected with *Staphylococcus aureus*, (**C and D**) The gene expression of inflammatory mediators and antibacterial were analyzed by qRT-PCR, (**E**) Body weight change curve of mice pretreated with BG for one week, followed by colitis induction with 3% DSS (n = 18-25), (**F and G**) Changes of colon length from (**E**), (**H**) FITC-dextran assay assessing intestinal barrier function (n = 5-11). Data are presented as mean ± SD. Statistical significance: *$p < 0.05$, ***$p < 0.001$; ****$p < 0.0001$. ns, not significant.

Fig S2. BG pretreatment 4 or 7 weeks ameliorates DSS-induced colitis.

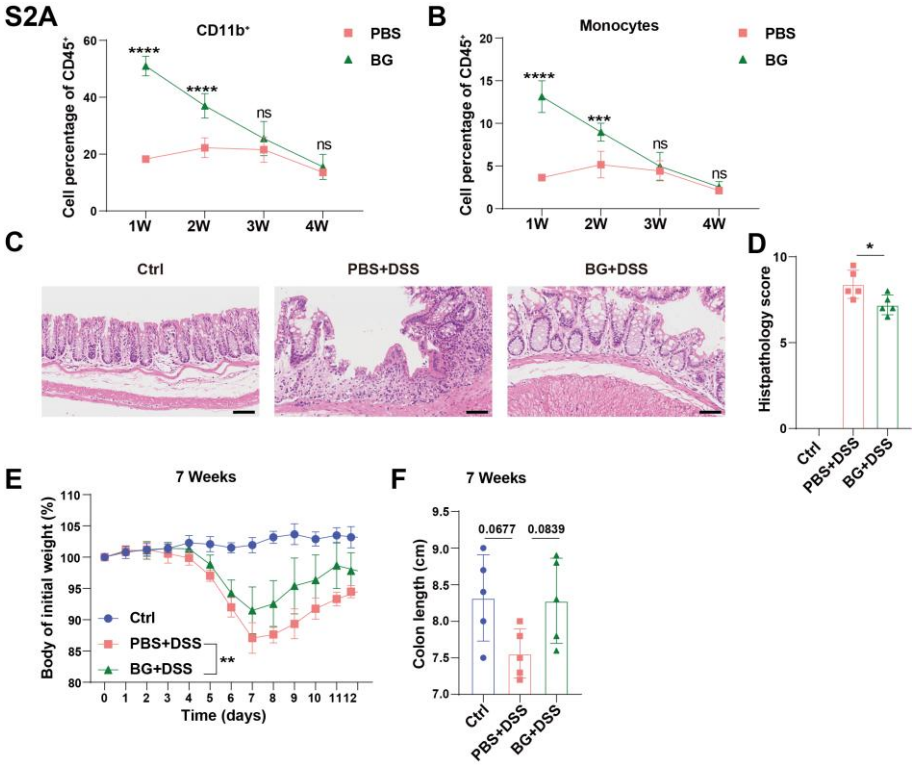

(**A and B**) Percentage of myeloid cells and monocytes in the peripheral blood of mice at different time points after one week of BG pretreatment, (**C and D**) H&E staining, and histological scoring of colitis mice after four weeks of BG training. Scale bars: 100 μm, (**E**) Body weight change curve of mice pretreated with BG for seven weeks, followed by colitis induction with 3% DSS, (**F**) Changes of colon length from (**E**) (n = 5). Data are presented as mean ± SD. Statistical significance: *$p < 0.05$, **$p < 0.01$, ***$p < 0.001$, ****$p < 0.0001$. ns, not significant.

Fig S3. BG pretreatment ameliorates colitis is independent of adaptive immunity.

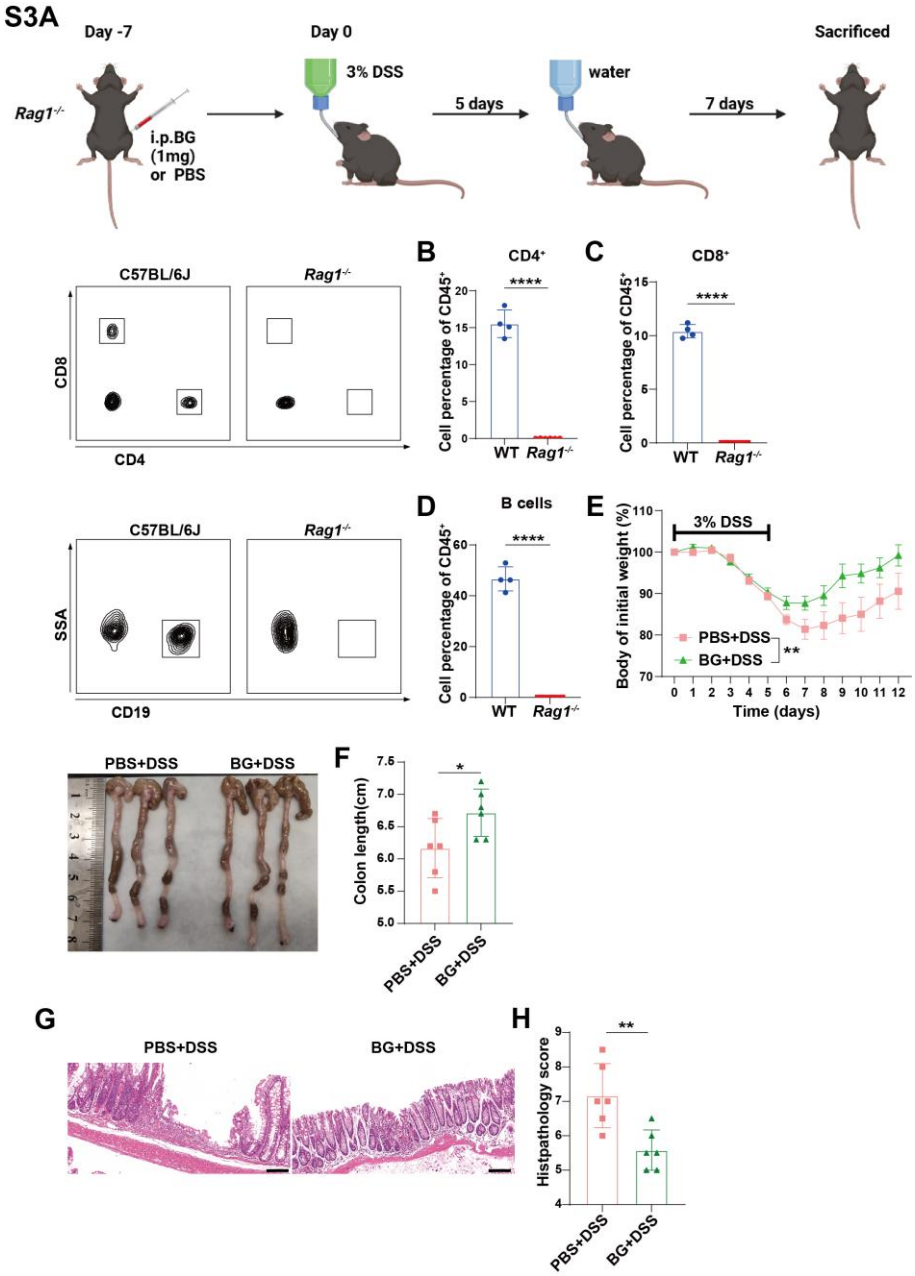

(**A**) Schematic representation of BG-induced trained immunity and DSS colitis model in *Rag1*$^{-/-}$ mice, (**B-D**) Flow cytometry analysis of peripheral blood from *Rag1*$^{-/-}$ mice, (**E**) Body weight change curve of *Rag1*$^{-/-}$ mice pretreated with BG for one week, followed by colitis induction with 3% DSS, (**F**) Colon length changes in *Rag1*$^{-/-}$ mice from (**E**), (**G and H**) H&E staining and histological scoring. Scale bars: 100 μm. Data are presented as mean ± SD. Statistical significance: *$p < 0.05$, **$p < 0.01$, ****$p < 0.0001$.

Fig S4. BG ameliorates colitis by enhancing myeloid cell activation.

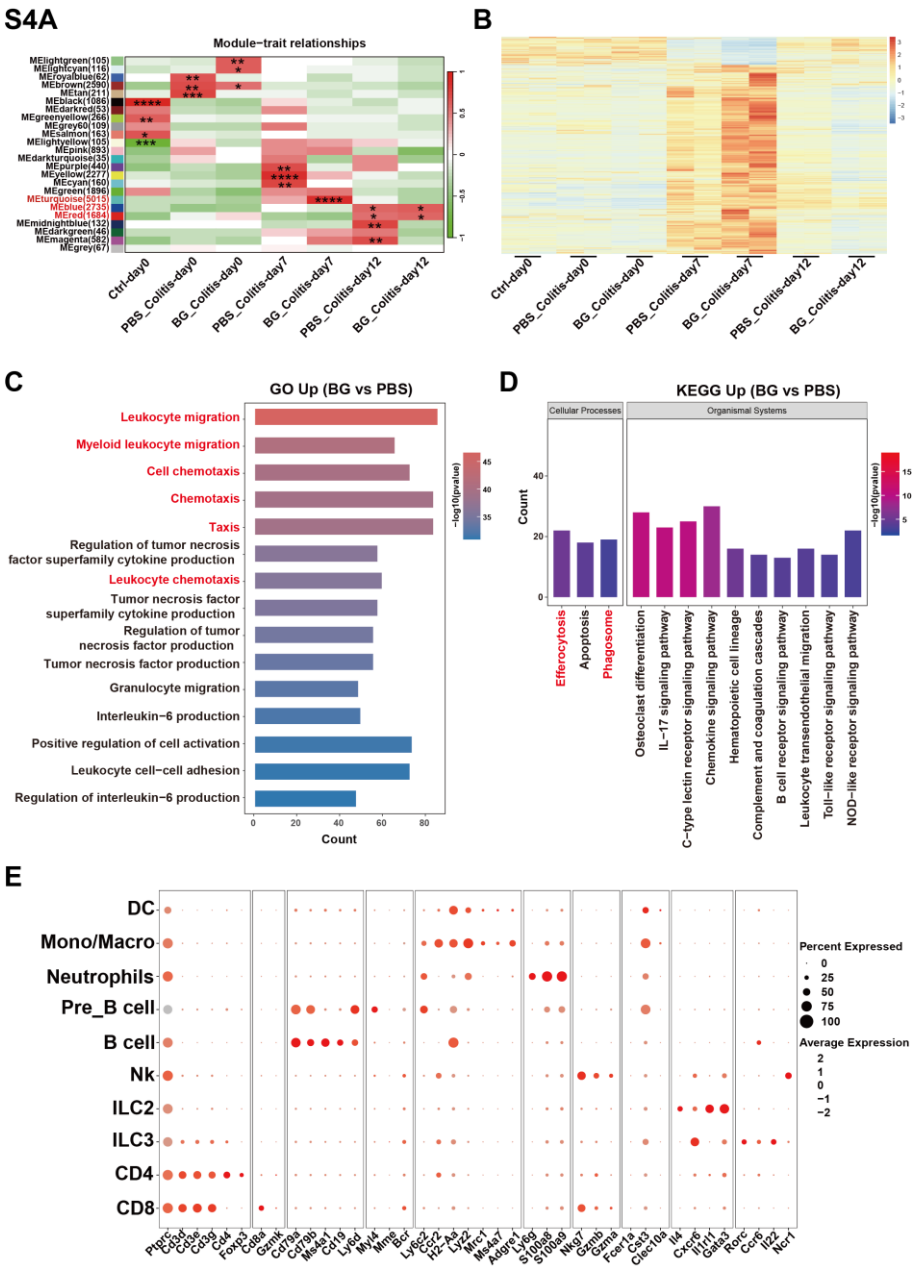

(**A**) RNA sequencing of colon tissue at different time points during colitis, with WGCNA identifying major gene modules, (**B**) DEGs in the Meturquoise module, (**C and D**) GO and KEGG pathway analysis of colon tissue on day seven of colitis after one week of BG pretreatment, (**E**) Expression of marker genes in LP CD45^{+} cells on day seven of colitis after one week of BG pretreatment.

Fig S5. BG trained bone marrow monocytes protected against colitis via the Ccl2-Ccr2 axis.

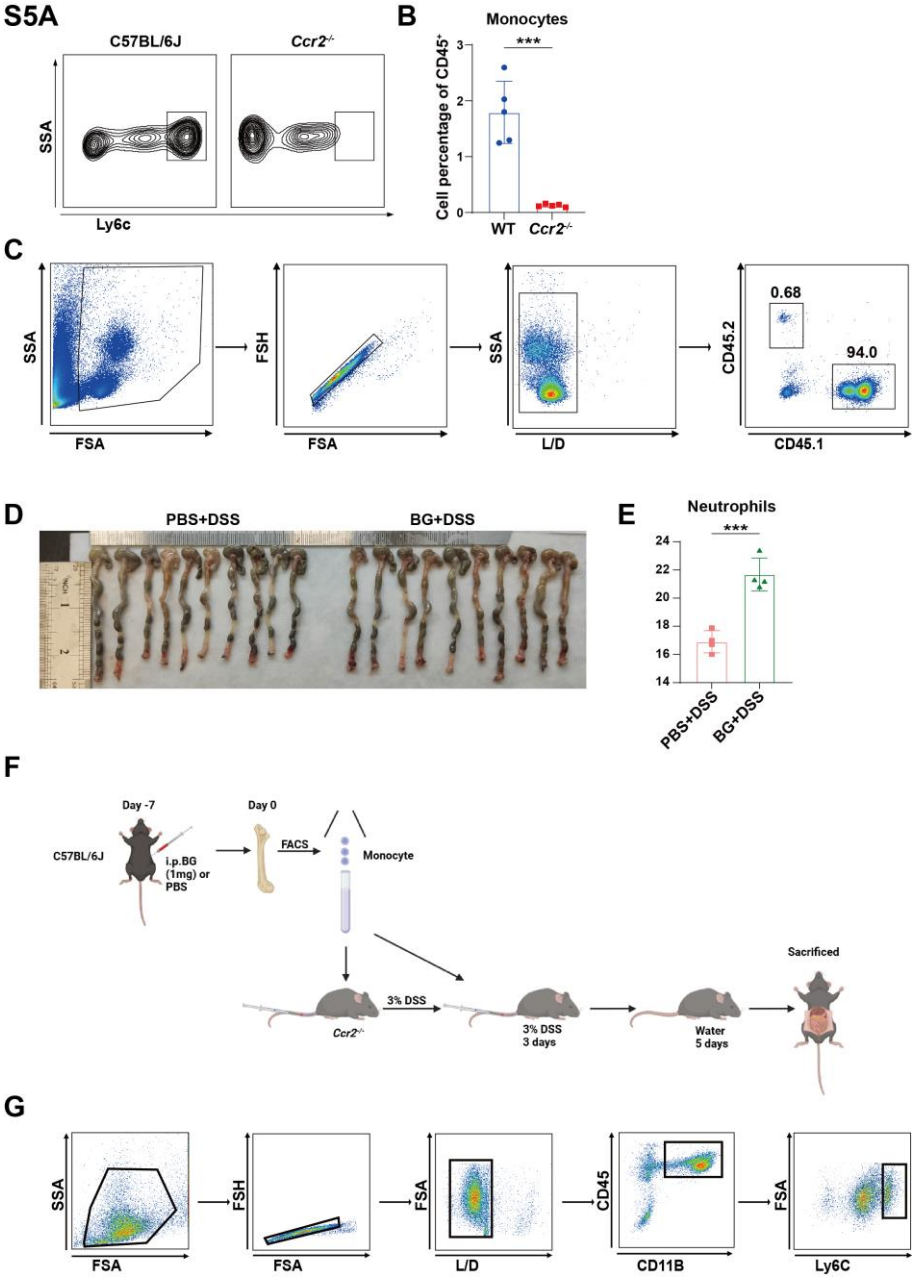

(**A and B**) Flow cytometry analysis of peripheral blood from *Ccr2*$^{-/-}$ mice, (**C**) Flow cytometry analysis of bone marrow reconstitution in CD45.2 recipient mice, (**D**) Colon length changes in bone marrow transplantation experiments from BG-pretreated CD45.1 mice to CD45.2 mice, (**E**) Percentage of Ly6G^{+} neutrophils in peripheral blood of CD45.2 recipient mice, (**F**) Bone marrow

monocytes transplant model, (**G**) Flow sorting scheme of bone marrow monocytes. Data are presented as mean ± SD. Statistical significance: ***$p < 0.001$.

Fig S6. BG pretreatment enhances innate immunity and phagocytic capacity.

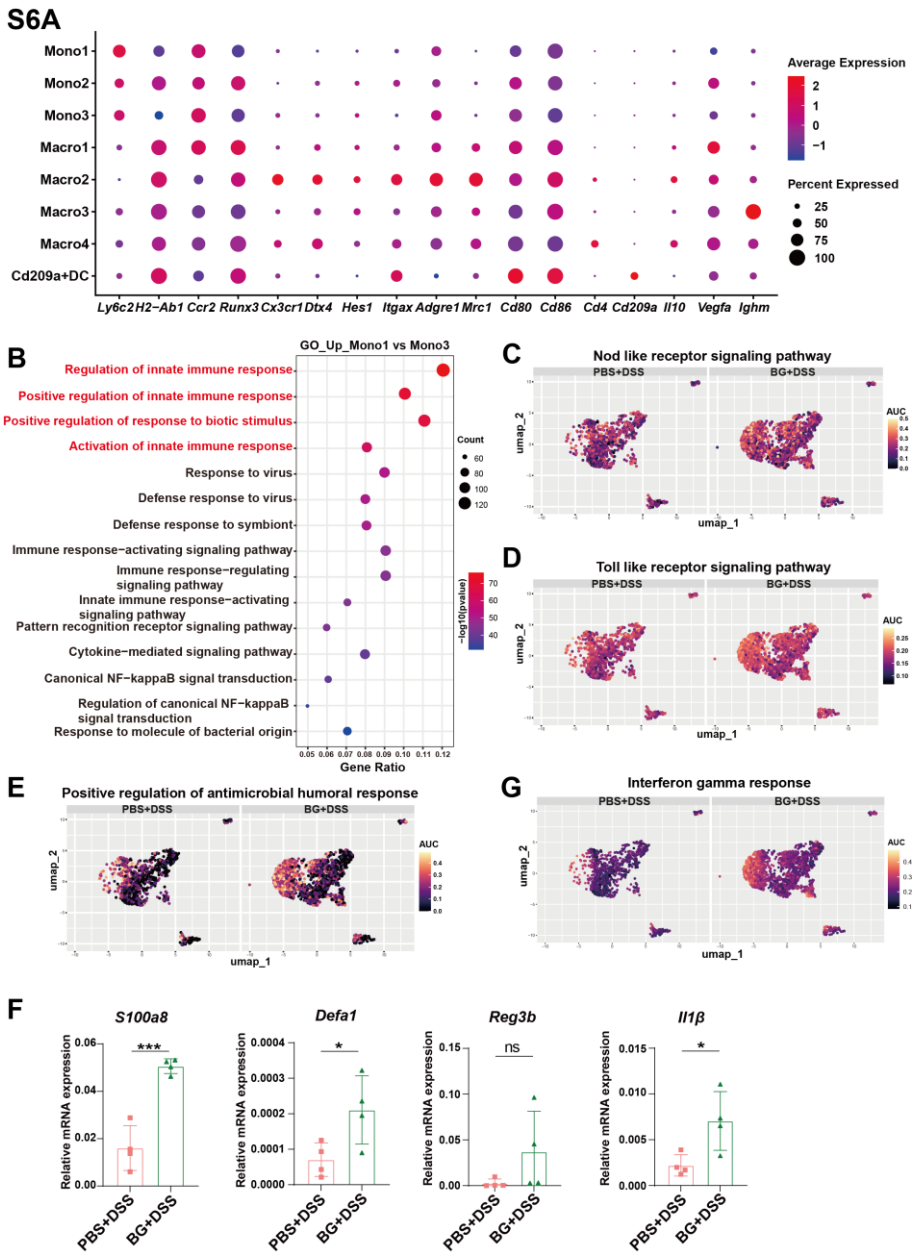

(**A**) Major marker genes of eight cell clusters within the monocyte/macrophage lineage, (**B**) GO analysis of genes upregulated in monocytes 1 and monocyte 3, (**C-E**) AUC scores of selected pathways, (**F**) Antibacterial gene expression was analyzed by qRT-PCR. (**G**) AUC scores of

selected pathways. Data are presented as mean ± SD. Statistical significance: *$p < 0.05$, ***$p < 0.001$, ns, not significant.

Fig S7. BG-induced trained immunity promotes monocyte differentiation.

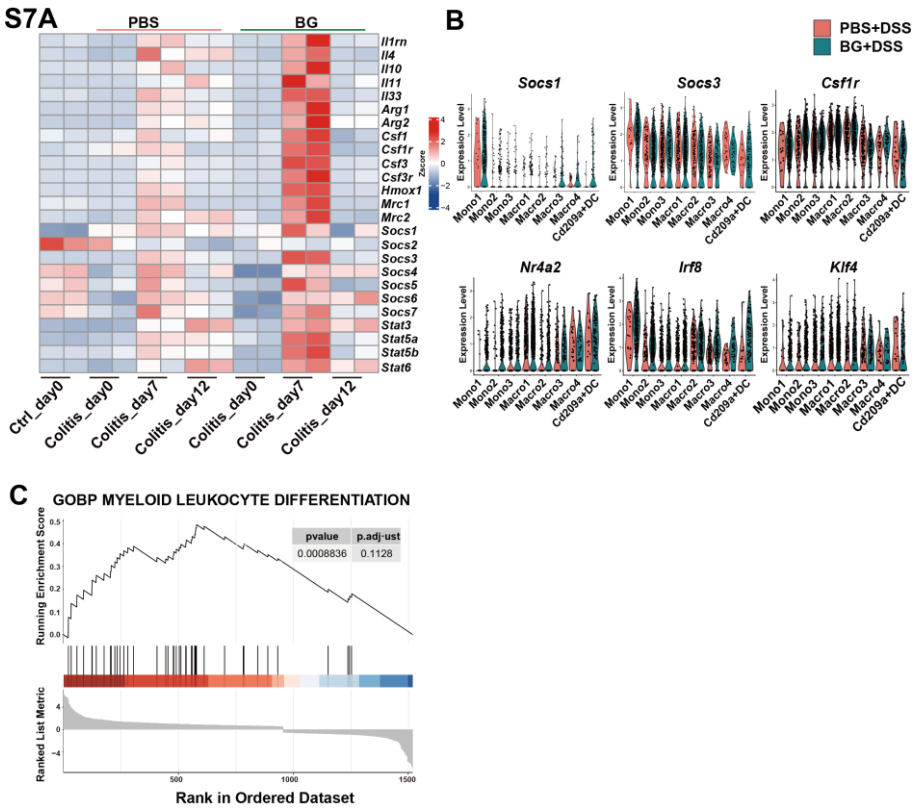

(**A**) Gene expression analysis at different time points of colitis, based on colon RNA sequencing, (**B**) Violin plots of gene expression in eight cell clusters, (**C**) GSEA analysis showing gene enrichment pattern on day seven of colitis.

Fig S8 BG training downregulates the proportion of peripheral monocytes during colitis development.

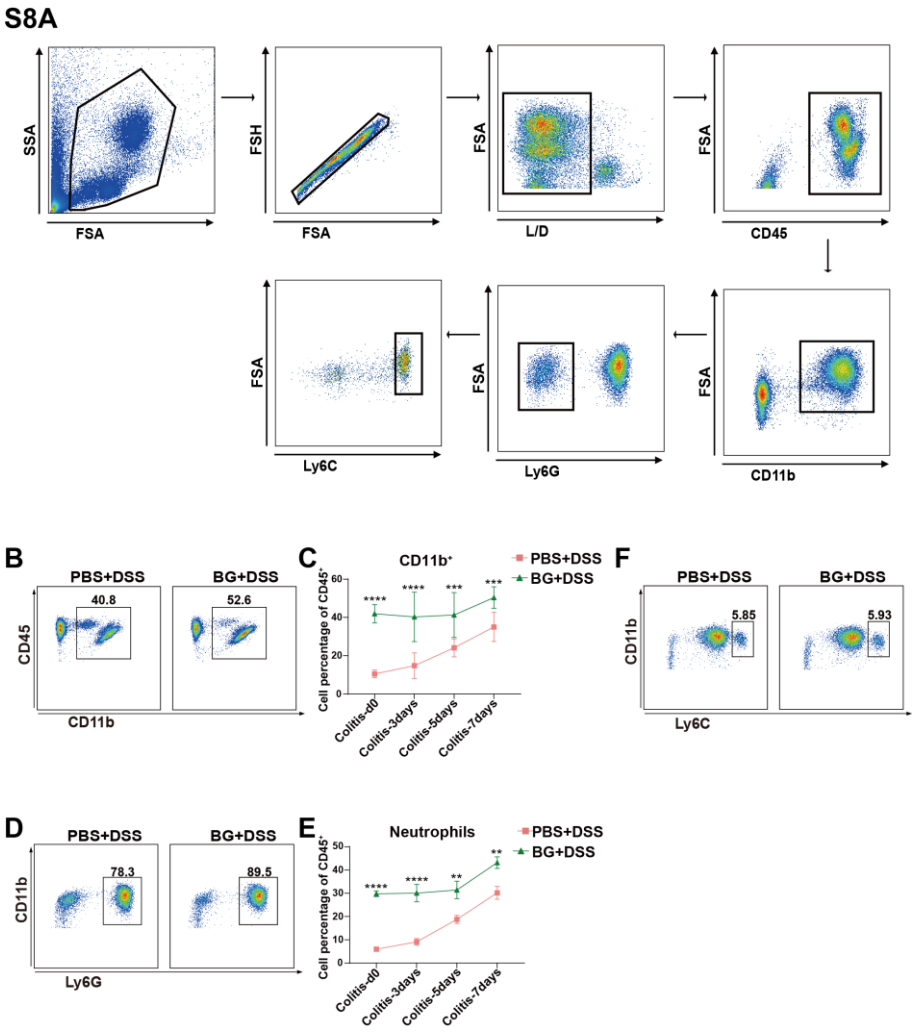

(**A**) Peripheral blood flow cytometry gating strategy, (**B**) Representative flow cytometry plots of $CD11b^+$ myeloid cells in peripheral blood on day seven of colitis (**C**) The percentage of $CD11b^+$ myeloid cells at different time points of colitis, (**D**) Representative flow cytometry plots of $Ly6G^+$ neutrophils in peripheral blood on day seven of colitis, (**E**) Percentage of $Ly6G^+$ neutrophils at different time points of colitis, (**F**) Representative flow cytometry plots of $Ly6C^{hi}$ monocytes in peripheral blood on day seven of colitis. Data are presented as mean ± SD. Statistical significance: $^{**}p < 0.01$; $^{***}p < 0.001$; $^{****}p < 0.0001$.

Fig S9 BG training upregulates the proportion of colonic monocytes/macrophages in colitis mice.

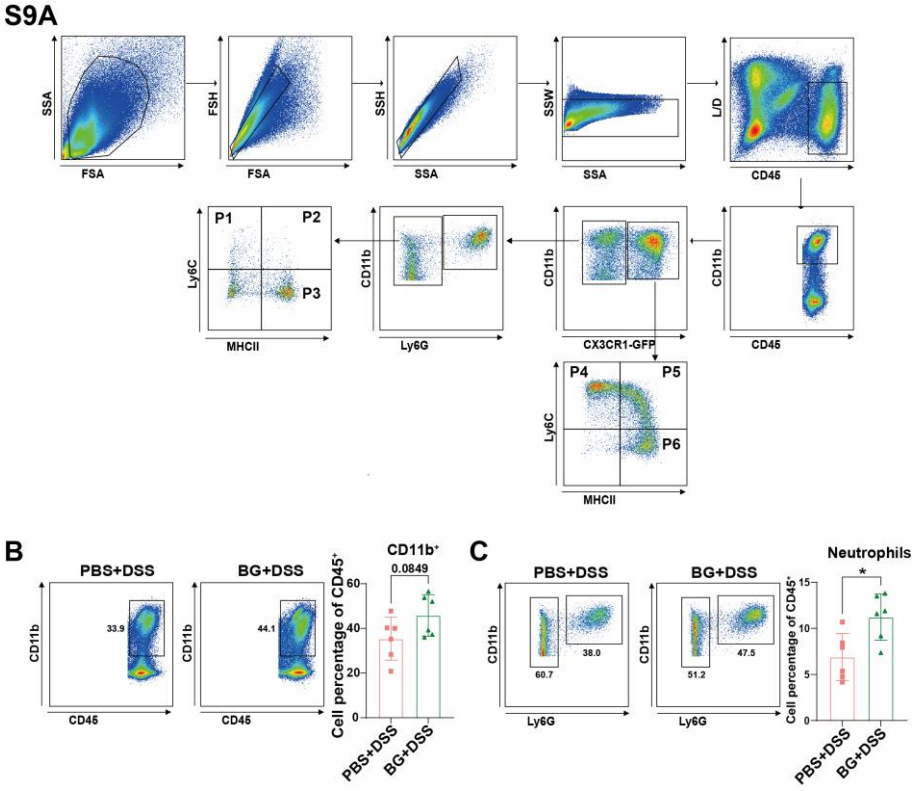

(**A**) Colonic LPMCs flow cytometry gating strategy, (**B and C**) The percentages of CD11b$^+$ myeloid cells (**B**) and Ly6G$^+$ neutrophils (**C**) were analyzed on day seven of colitis (n = 6). Data are presented as mean ± SD. Statistical significance: *p < 0.05. ns, not significant.

Fig S10 Adoptive transfer of BG-trained monocytes ameliorates experimental colitis.

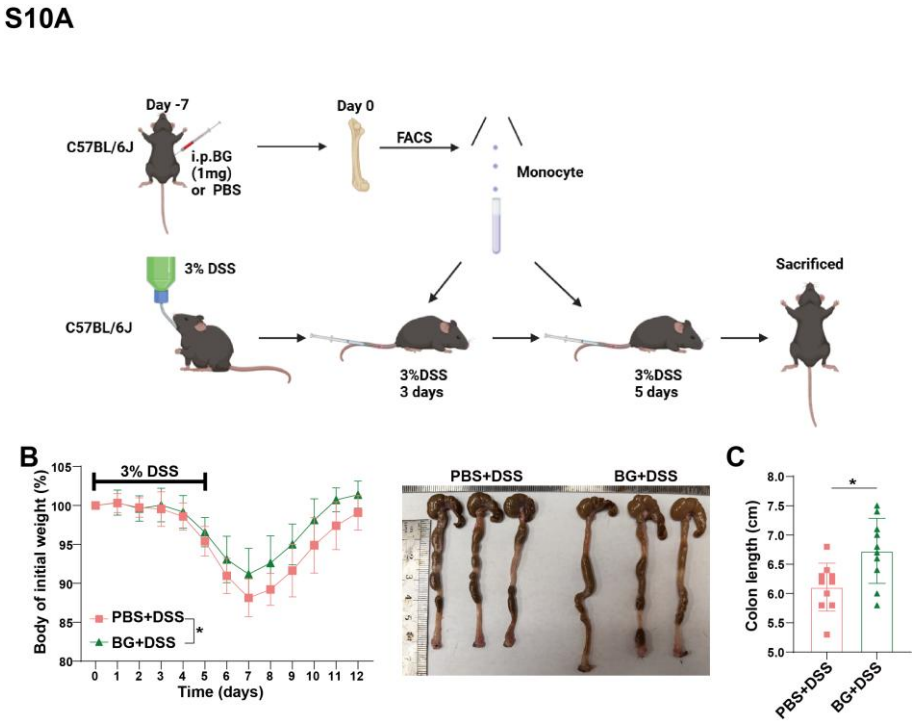

(**A**) Bone marrow monocytes transplant and colitis treatment model, (**B and C**) Body weight change curve (**B**) and colon length changes (**C**) in WT colitis mice receiving Ly6C^{hi} monocyte adoptive transfer (n = 10). Data are presented as mean ± SD. Statistical significance: *p < 0.05.